Results in Physics 31 (2021) 105036

Contents lists available at ScienceDirect

Results in Physics

journal homepage: www.elsevier.com/locate/rinp

Extracting novel categories of analytical wave solutions to a nonlinear Schrödinger equation of unstable type

Yan Cao [a], Hayder A. Dhahad [b], Fahd Jarad [c,d,*], Kamal Sharma [e], Ali A. Rajhi [f], A.S. El-Shafay [g,h], Shima Rashidi [i], Shahram Rezapour [j,*], S.A. Najati [k], Ayman A. Aly [l], Abdulaziz H. Alghtani [l], Muhammad Bilal Riaz [m,n,**]

[a] School of Mechatronic Engineering, Xi'an Technological University, Xi'an, 710021, China
[b] Mechanical Engineering Department, University of Technology, Baghdad, Iraq
[c] Department of Mathematics, Cankaya University, Etimesgut 06790, Ankara, Turkey
[d] Department of Medical Research, China Medical University, Taichung 40402, Taiwan
[e] Institute of Engineering and Technology, GLA University, Mathura (U.P.), 281406, India
[f] Department of Mechanical Engineering, College of Engineering, King Khalid University, PO Box 394, Abha 61421, Saudi Arabia
[g] Department of Mechanical Engineering, College of Engineering, Prince Sattam bin Abdulaziz University, Alkharj 11942, Saudi Arabia
[h] Department of Mechanical Power Engineering, Faculty of Engineering, Mansoura University, Egypt
[i] Department of Computer Science, College of Science and Technology, University of Human Development, Sulaimani, Kurdistan Region, Iraq
[j] Department of Medical Research, China Medical University Hospital, China Medical University, Taichung, Taiwan
[k] Department of Mathematics and Statistics, College of Science, Taif University, P.O. Box 11099, Taif 21944, Saudi Arabia
[l] Department of Mechanical Engineering, College of Engineering, Taif University, P.O. Box 11099, Taif 21944, Saudi Arabia
[m] Department of Automation, Biomechanics and Mechatronics, Lodz University of Technology, 1/15 8 Stefanowskiego St., 90-924, Lodz, Poland
[n] Department of Mathematics, University of Management and Technology, Lahore, Pakistan

ARTICLE INFO

Keywords:
Unstable nonlinear Schrödinger equation
Traveling wave solutions
Optical fibers
Nonlinear algebraic system

ABSTRACT

Solving partial differential equations has always been one of the significant tools in mathematics for modeling applied phenomena. In this paper, using an efficient analytical technique, exact solutions for the unstable Schrödinger equation are constructed. This type of the Schrödinger equation describes the disturbance of time period in slightly stable and unstable media and manages the instabilities of lossless symmetric two stream plasma and two layer baroclinic. The basis of this method is the generalization of some commonly used methods in the literature. To better demonstrate the results, we perform many numerical simulations corresponding to the solutions. All these solutions are new achievements for this form of the equation that have not been acquired in previous research. As one of the strengths of the article, it can be pointed out that not only is the method very straightforward, but also can be used without the common computational complexities observed in known analytical methods. In addition, during the use of the method, an analytical solution is obtained in terms of familiar elementary functions, which will make their use in practical applications very convenient. On the other hand, the utilized methodology empowers us to handle other types of well-known models. All numerical results and simulations in this article have been obtained using computational packages in Wolfram Mathematica.

Introduction

Finding exact solutions for differential equations with partial derivatives has been one of the most important basic needs of researchers in various fields of science [1–24]. This importance has led to the introduction and use of several methods in this regard [25–45]. For example, the one-lump-multi-stripe and one-lump-multi-soliton solutions to nonlinear partial differential equations has been analyzed via Hirota bilinear forms in [46]. The authors in [47], have applied the Painlevé test has been conducted to reveal the Painlevé-integrability of a novel (2+1)-dimensional nonlinear model. Consequently, they

* Corresponding authors.
** Corresponding author at: Department of Automation, Biomechanics and Mechatronics, Lodz University of Technology, 1/15 8 Stefanowskiego St., 90-924, Lodz, Poland.
E-mail addresses: fahd@cankaya.edu.tr (F. Jarad), sh.rezapour@mail.cmuh.org.tw (S. Rezapour), muhammad.riaz@p.lodz.pl (M.B. Riaz).

https://doi.org/10.1016/j.rinp.2021.105036
Received 1 November 2021; Received in revised form 15 November 2021; Accepted 18 November 2021
Available online 23 November 2021

obtained several non-resonant soliton solutions, Bäacklund transformation, Lax pair and infinitely many conservation laws. The work in [48] presents an optional decoupling condition approach is proposed for deriving the lump-stripe solutions and lump-soliton solutions to the KPI equation where the authors have proved there exists a link between the two kinds of interaction solutions. Taking the Hirota bilinear method and symbolic computation into account the authors in [49] investigated the (3 + 1)-dimensional generalized Kadomtsev–Petviashvili equation. Based on its bilinear form, the bilinear Bäcklund transformation. Then, they obtained the Pfaffian, Wronskian and Grammian form solutions are derived via the properties of determinant. Based on the (2+1)- dimensional Burgers model, a generalized variable-coefficient Burgers equation is introduced in [50]. Then, some lump solutions to the generalized Burgers equation with variable coefficients were extracted in the same reference. The Sine–Gordon expansion method has used in [51] to study the coupled conformable Fokas–Lenells equation with spatio-temporal dispersion. Moreover, several solitary wave ansatzs are utilized in [52] to study exact solutions for a weakly nonlocal Schrödinger equation of the fifth order involving nonlinearity of the parabolic law and an external potential. Consequently, they successfully derived several bright, dark, singular, periodic soliton and exponential solutions for the model. The Riccati equation, Kudryashov and a new auxiliary ordinary differential equation method are three utilized integration techniques used in [53] to solve the Lakshmanan–Porsezian–Daniel (LPD) model with Kerr nonlinearity using Bäcklund transformation. Further, the work in [54] has considered the extended rational sinh–cosh method (ERSCM) and modified Khater method to solve the biological population model to derive new exact solutions. In [54], the traveling wave solutions to the (2 + 1)-dimensional dispersive long wave equation are determined via the (G'/G)-expansion method. One of the biggest challenges in this direction is that it may not be possible to find exact solutions to some of the equations. In these cases, the use of approximate and numerical methods is recommended. These techniques are also quite popular and wildly used [55–80]. In recent decades, researchers have tried to provide new and more effective definitions for the concept of derivative. An important reason for the need for these activities is that standard derivatives may lose their efficiency in the accurate description of some phenomena. The result of these efforts is the provision of several definitions for non-integer order derivatives, which are natural extensions for standard integer-order derivatives. Some of these definitions include the Conformable derivative [81], β-derivative [82], Caputo fractional derivative [83], Riemann–Liouville fractional derivatives [84], Caputo–Fabrizio fractional derivative [85], Atangana–Baleanu fractional derivative [86]. There is a wide range of practical applications for each of these derivatives [87–113]. This level of efficiency and importance has led to continuous and uninterrupted efforts to advance these definitions and address potential shortcomings. In this paper, we aim to study a variety of Schrödinger's equation called unstable nonlinear Schrödinger's equation given by [114–116]

$$i\frac{\partial \mathscr{Q}(x,t)}{\partial t}+\frac{\partial^2 \mathscr{Q}(x,t)}{\partial x^2}+2\lambda|\mathscr{Q}(x,t)|^2\mathscr{Q}(x,t)-\gamma\frac{\partial^2 \mathscr{Q}(x,t)}{\partial x\partial t}=0. \tag{1}$$

In this model λ and γ are arbitrary real constants, and the dependent variable $\mathscr{Q}(x,t)$ is independent variables of x and t as spatial and temporal variables respectively. This form of Schrödinger's equation is utilized while modeling the problems in two-layer baroclinic instability and the lossless symmetric two-stream plasma instability when a time evolution of disturbances in marginally stable or unstable media [114]. This fundamental change in the equation provides access to new sets of analytical solutions to this equation. In addition, more theories and applications of the unstable nonlinear Schrödinger equation can be found in [117]. The high importance of this equation in different applications has led to the use of different methods in determining analytical solutions for this equation. For example, the extended simple equation method has been utilized in [118] to construct exact traveling wave solutions of the equation. The unstable nonlinear Schrödinger equation has been investigated in [119] via a new version of the trial equation method. Arshad et al. [120] utilized a modified extended mapping method to construct different forms of the exact solutions of the equation such as exact dark soliton, exact bright soliton, bright–dark soliton, solitary wave, elliptic function in different form, and periodic solutions to Eq. (1). In [121], the authors have supposed several ansatz functions for the solution of the equation. And they have introduced many different solutions to the equation. Several explicit new exact solutions such as soliton, solitary wave, elliptic function and periodic solutions of unstable NLSE are constructed in [122] by using the proposed modified extended mapping method. Novel exact wave solutions to the equation, have been also proposed in [123] via the modified exponential rational function method. The work of [124] presents several lumps, lump with one kink, lump with two kink, rogue wave, and lump interactions with periodic and kink solitons for the equation using diverse ansatz transformations. Along with the research work done above, this paper aims to retrieve several wave solutions to the unstable nonlinear Schrödinger's Eq. (1) via an efficient methodology. So, we organize the article as follows: In Section "The solution procedure", a systematic description of the solution procedure is stated. The application of the method to find new wave solutions to Eq. (1) along with their corresponding numerical simulations are presented in Section "The main results". In this section, the sensitivity of the system will be also measured in terms of changes in two fixed parameters in the model by drawing some 2D diagrams. Finding these novel solutions is the main achievement of our present contribution. Then finally, the paper is concluded by stating some remarkable results in the last section.

The solution procedure

Taking into account the following new transformation

$$\zeta=\kappa x-\omega t,\quad \Phi(x,t)=\sigma x+\mu t, \tag{2}$$

we assume that Eq. (1) has a solution in the following structure

$$\mathscr{Q}(x,t)=\mathscr{Q}(\zeta)e^{i\Phi(x,t)}, \tag{3}$$

where κ,ω,σ and μ are unknown constants.

Now, we utilize the wave transformation (2) in Eq. (1) and set the coefficients of real and imaginary parts in resultant to zero. Then, we obtain $\omega=\frac{\kappa(\gamma\mu-2\sigma)}{\gamma\sigma-1}$, and

$$2\lambda\mathscr{Q}^3(\zeta)+\left(\gamma\mu\sigma-\mu-\sigma^2\right)\mathscr{Q}(\zeta)+\kappa\left(\gamma\omega+\kappa\right)\frac{d^2\mathscr{Q}(\zeta)}{d\zeta^2}=0. \tag{4}$$

Now, taking $\Lambda_1=2\lambda$, $\Lambda_2=\gamma\mu\sigma-\mu-\sigma^2$, $\Lambda_3=\kappa\left(\gamma\omega+\kappa\right)$ into account in (4), we can write

$$\Lambda_1\mathscr{Q}^3(\zeta)+\Lambda_2\mathscr{Q}(\zeta)+\Lambda_3\frac{d^2\mathscr{Q}(\zeta)}{d\zeta^2}=0. \tag{5}$$

Now, through the application logarithmic transformation $\mathscr{Q}=2\left(\ln(\mathrm{q}(\zeta))\right)_\zeta$ in (5), the equation is expanded as follows

$$\begin{aligned}&\Lambda_3\left(\frac{\partial^3\mathrm{q}(\zeta)}{\partial\zeta^3}\right)\mathrm{q}^2(\zeta)-3\Lambda_3\mathrm{q}(\zeta)\left(\frac{\partial^2\mathrm{q}(\zeta)}{\partial\zeta^2}\right)\left(\frac{\partial\mathrm{q}(\zeta)}{\partial\zeta}\right)+2\Lambda_3\left(\frac{\partial\mathrm{q}(\zeta)}{\partial\zeta}\right)^3\\&+\Lambda_2\left(\frac{\partial\mathrm{q}(\zeta)}{\partial\zeta}\right)\mathrm{q}^2(\zeta)+4\Lambda_1\left(\frac{\partial\mathrm{q}(\zeta)}{\partial\zeta}\right)^3=0.\end{aligned} \tag{6}$$

To search for the solution to Eq. (5) in terms of exponential functions, let us consider the following general structure for the solution

$$\mathrm{q}(\zeta)=\rho_0+\frac{\rho_1e^{\alpha_1\zeta+\beta_1}+\rho_2e^{\alpha_2\zeta+\beta_2}}{\rho_3e^{\alpha_3\zeta+\beta_3}+\rho_4e^{\alpha_4\zeta+\beta_4}}+\left(\frac{\rho_1e^{\alpha_1\zeta+\beta_1}+\rho_2e^{\alpha_2\zeta+\beta_2}}{\rho_3e^{\alpha_3\zeta+\beta_3}+\rho_4e^{\alpha_4\zeta+\beta_4}}\right)^{-1}, \tag{7}$$

where $\rho_0,\rho_1,\rho_2,\rho_3,\rho_4$ and $\alpha_1,\alpha_2,\alpha_3,\alpha_4,\beta_1,\beta_2,\beta_3,\beta_4$ are unknown parameters need to be determine.

To determine the analytical solution to Eq. (5), we substitute Eq. (7) into Eq. (6). Then, we arrive to a polynomial equation $P(\nu_1,\nu_2,\nu_3,\nu_4)=$

$$\mathscr{Q}(\zeta)=\frac{2\left(\alpha_2-\alpha_4\right)\left(\rho_1 e^{\zeta\alpha_2+\beta_1}+\rho_2 e^{\zeta\alpha_2+\beta_2}+\rho_3 e^{\zeta\alpha_4+\beta_3}+\rho_4 e^{\zeta\alpha_4+\beta_4}\right)\left(\rho_1 e^{\zeta\alpha_2+\beta_1}+\rho_2 e^{\zeta\alpha_2+\beta_2}-\rho_3 e^{\zeta\alpha_4+\beta_3}-\rho_4 e^{\zeta\alpha_4+\beta_4}\right)}{\left(e^{\zeta\alpha_2+\beta_1}\right)^2\rho_1^2+2\,e^{\zeta\alpha_2+\beta_1}e^{\zeta\alpha_2+\beta_2}\rho_1\rho_2+\left(e^{\zeta\alpha_2+\beta_2}\right)^2\rho_2^2+\left(\rho_3 e^{\zeta\alpha_4+\beta_3}+\rho_4 e^{\zeta\alpha_4+\beta_4}\right)^2}.$$

Box I.

$$\mathscr{Q}_1(x,t)=\frac{2\left(\alpha_2-\alpha_4\right)\left(\rho_1 e^{\zeta\alpha_2+\beta_1}+\rho_2 e^{\zeta\alpha_2+\beta_2}+\rho_3 e^{\zeta\alpha_4+\beta_3}+\rho_4 e^{\zeta\alpha_4+\beta_4}\right)\left(\rho_1 e^{\zeta\alpha_2+\beta_1}+\rho_2 e^{\zeta\alpha_2+\beta_2}-\rho_3 e^{\zeta\alpha_4+\beta_3}-\rho_4 e^{\zeta\alpha_4+\beta_4}\right)}{\left(e^{\zeta\alpha_2+\beta_1}\right)^2\rho_1^2+2\,e^{\zeta\alpha_2+\beta_1}e^{\zeta\alpha_2+\beta_2}\rho_1\rho_2+\left(e^{\zeta\alpha_2+\beta_2}\right)^2\rho_2^2+\left(\rho_3 e^{\zeta\alpha_4+\beta_3}+\rho_4 e^{\zeta\alpha_4+\beta_4}\right)^2}\times e^{i\Phi(x,t)},\tag{10}$$

Box II.

0, in terms of $v_i=e^{\alpha_i\zeta+\beta_i}$ for i = 0.48, … , 4. Zeroing coefficients of variables in v_i introduces a system of nonlinear equations in terms of undetermined parameters of $\kappa,\sigma,\mu,\rho_0,\rho_1,\rho_2,\rho_3,\rho_4$ and $\alpha_1,\alpha_2,\alpha_3,\alpha_4,\beta_1,\beta_2,\beta_3,\beta_4$. After solving the resulting system, we insert its solutions into Eq. (7) and take $\mathscr{Q}=2\left(\ln(\mathrm{q}(\zeta))\right)_\zeta$ into account along with Eq. (3). Analytical solutions for the differential equation with partial derivatives (1) will then be extracted.

The main results

After pursuing the steps mentioned in the previous section, the following analytical solutions are constructed:

Category 1: In this case, we obtain

$$\kappa=\frac{2\sqrt{\left(8\gamma^2\lambda\alpha_2^2-16\gamma^2\lambda\alpha_2\alpha_4+8\gamma^2\lambda\alpha_4^2-1\right)\lambda}\,(\gamma\sigma-1)}{8\gamma^2\lambda\alpha_2^2-16\gamma^2\lambda\alpha_2\alpha_4+8\gamma^2\lambda\alpha_4^2-1},\ \mu=-\frac{8\lambda\alpha_2^2-16\alpha_4\lambda\alpha_2+8\alpha_4^2\lambda-\sigma^2}{\gamma\sigma-1},$$
$$\sigma=\sigma,\alpha_1=\alpha_2,\alpha_2=\alpha_2,\alpha_3=\alpha_4,\alpha_4=\alpha_4,$$
$$\beta_1=\beta_1,\beta_2=\beta_2,\beta_3=\beta_3,\beta_4=\beta_4,\rho_0=0,\rho_1=\rho_1,\rho_2=\rho_2,\rho_3=\rho_3,\rho_4=\rho_4.\tag{8}$$

provided that $\left(8\gamma^2\lambda\alpha_2^2-16\gamma^2\lambda\alpha_2\alpha_4+8\gamma^2\lambda\alpha_4^2-1\right)\lambda>0$.

If we employ the these values in Eq. (7) one gets

$$\mathrm{q}(\zeta)=\frac{\rho_1 e^{\zeta\alpha_2+\beta_1}+\rho_2 e^{\zeta\alpha_2+\beta_2}}{\rho_3 e^{\zeta\alpha_4+\beta_3}+\rho_4 e^{\zeta\alpha_4+\beta_4}}+\frac{\rho_3 e^{\zeta\alpha_4+\beta_3}+\rho_4 e^{\zeta\alpha_4+\beta_4}}{\rho_1 e^{\zeta\alpha_2+\beta_1}+\rho_2 e^{\zeta\alpha_2+\beta_2}}.\tag{9}$$

So, it reads as given in Box I.

Accordingly, the analytical solution in this case, is structured as (see Eq. (10) given as in Box II)

where

$$\zeta=\frac{\sqrt{8}\sqrt{\lambda\left(-\frac{1}{8}+\gamma^2(\alpha_2-\alpha_4)^2\lambda\right)}\left(\gamma^2\sigma^2x+\left(8t(\alpha_2-\alpha_4)^2\lambda+\sigma^2t-2\sigma x\right)\gamma-2\sigma t+x\right)}{4(\gamma\sigma-1)\left(-\frac{1}{8}+\gamma^2(\alpha_2-\alpha_4)^2\lambda\right)},$$
$$\Phi=-\frac{\left(8\lambda\alpha_2^2-16\alpha_4\lambda\alpha_2+8\alpha_4^2\lambda-\sigma^2\right)t}{\gamma\sigma-1}+\sigma x.\tag{11}$$

Moreover, solution (10) covers abundant analytical solutions for the main equation, which are described below.

Sub-family 1: Considering the case of $\gamma=2,\lambda=2,\gamma=2,\lambda=2,\sigma=1,\alpha_2=\mathrm{i},\alpha_4=1+\mathrm{i},\beta_1=-\mathrm{i},\beta_2=-\mathrm{i},\beta_3=-\mathrm{i},\beta_4=-\mathrm{i},\rho_1=1,\rho_2=1,\rho_3=-2,\rho_4=-2$ in (10) yields the following analytical solution

$$\mathscr{Q}_{1,1}(x,t)=\frac{8\cosh\left(\frac{(128t+4x)\sqrt{14}}{21}\right)+8\sinh\left(\frac{(128t+4x)\sqrt{14}}{21}\right)-2}{4\cosh\left(\frac{(128t+4x)\sqrt{14}}{21}\right)+4\sinh\left(\frac{(128t+4x)\sqrt{14}}{21}\right)+1}\times e^{\mathrm{i}(-15t+x)}.\tag{12}$$

Sub-family 2: Taking the case of $\gamma=2,\lambda=2,\sigma=1,\alpha_2=1,\alpha_4=-1,\beta_1=-1,\beta_2=-1,\beta_3=-1,\beta_4=-1,\rho_1=1,\rho_2=1,\rho_3=-2,\rho_4=-2$ into account in (10) yields the following analytical solution, see Eq. (13) given as in Box III

where $\Phi=-63t+x$.

Through considering $\alpha_1=0.48,\alpha_2=0.1,\alpha_3=0.8,\alpha_4=0.7,\beta_1=0.48,\beta_2=0.48,\beta_3=0.48.5,\beta_4=0.48,\rho_1=0.48,\rho_2=0.75,\rho_3=0.9,\rho_4=0.2$, and $\sigma=2,\lambda=2.94,\gamma=2.94$ in (10) the resulted dynamic behavior related to the analytical solution obtained have been also displayed in Fig. 1. In addition, the sensitivity of this solution is demonstrated based on the changes of two parameters λ and γ in Figs. 2 and 3, respectively. In these diagrams, it can be seen that increasing the value of the parameters will make the solutions more stable in the considered conditions.

Category 2: In this case, we obtain

$$\kappa=\frac{4\sqrt{\left(8\gamma^2\lambda\alpha_1^2-16\gamma^2\lambda\alpha_1\alpha_4+8\gamma^2\lambda\alpha_4^2-1\right)\lambda}\,(\gamma\sigma-1)}{8\gamma^2\lambda\alpha_1^2-16\gamma^2\lambda\alpha_1\alpha_4+8\gamma^2\lambda\alpha_4^2-1},\ \mu=-\frac{8\lambda\alpha_1^2-16\alpha_4\lambda\alpha_1+8\alpha_4^2\lambda-\sigma^2}{\gamma\sigma-1},$$
$$\sigma=\sigma,\alpha_1=\alpha_1,\alpha_2=\alpha_2,\alpha_3=\alpha_3,\alpha_4=\alpha_4,$$
$$\beta_1=\beta_1,\beta_2=\beta_2,\beta_3=\beta_3,\beta_4=\beta_4,\rho_0=-2,\rho_1=\rho_1,\rho_2=0,\rho_3=0,\rho_4=\rho_4.\tag{14}$$

Inserting these values into Eq. (7) yields

$$\mathrm{q}(\zeta)=\frac{\left(\rho_1 e^{\zeta\alpha_1+\beta_1}-\rho_4 e^{\zeta\alpha_4+\beta_4}\right)^2}{\rho_4 e^{\zeta\alpha_4+\beta_4}\rho_1 e^{\zeta\alpha_1+\beta_1}}.\tag{15}$$

Therefore, it reads

$$\mathscr{Q}(\zeta)=\frac{2\left(\alpha_1-\alpha_4\right)\left(\rho_1 e^{\zeta\alpha_1+\beta_1}+\rho_4 e^{\zeta\alpha_4+\beta_4}\right)}{\rho_1 e^{\zeta\alpha_1+\beta_1}-\rho_4 e^{\zeta\alpha_4+\beta_4}}.$$

Finally, the analytical solution in this case, is structured as follows

$$\mathscr{Q}_2(x,t)=\frac{2\left(\alpha_1-\alpha_4\right)\left(\rho_1 e^{\zeta\alpha_1+\beta_1}+\rho_4 e^{\zeta\alpha_4+\beta_4}\right)}{\rho_1 e^{\zeta\alpha_1+\beta_1}-\rho_4 e^{\zeta\alpha_4+\beta_4}}\times e^{i\Phi(x,t)},\tag{16}$$

where

$$\zeta=\frac{\sqrt{8}\sqrt{\lambda\left(-\frac{1}{8}+\gamma^2(\alpha_1-\alpha_4)^2\lambda\right)}\left(\gamma^2\sigma^2x+\left(8t(\alpha_1-\alpha_4)^2\lambda+\sigma^2t-2\sigma x\right)\gamma-2\sigma t+x\right)}{2(\gamma\sigma-1)\left(-\frac{1}{8}+\gamma^2(\alpha_1-\alpha_4)^2\lambda\right)},$$
$$\Phi=-\frac{\left(8\lambda\alpha_1^2-16\alpha_4\lambda\alpha_1+8\alpha_4^2\lambda-\sigma^2\right)t}{\gamma\sigma-1}+\sigma x.\tag{17}$$

Further, solution (16) covers abundant analytical solutions for the main equation, which are described below.

Sub-family 1: Considering the case of $\gamma=2,\lambda=1,\sigma=2,\alpha_1=1,\alpha_4=-1,\beta_1=-1,\beta_4=-1,\rho_1=1,\rho_4=-2$ in (16) yields the following analytical solution

$$\mathscr{Q}_{2,1}(x,t)=\frac{4\cosh(-\zeta)+4\sinh(-\zeta)-8\cosh(\zeta)+8\sinh(\zeta)}{\cosh(-\zeta)+\sinh(-\zeta)+2\cosh(\zeta)-2\sinh(\zeta)}\times e^{\mathrm{i}\Phi},\tag{18}$$

where $\zeta=0.48+\frac{(272t+36x)\sqrt{127}}{381},\Phi=-\frac{28t}{3}+2x$.

Sub-family 2: Considering the case of $\gamma=2,\lambda=1,\sigma=2,\alpha_1=\mathrm{i},\alpha_4=-1+\mathrm{i},\beta_1=-\mathrm{i},\beta_4=-\mathrm{i},\rho_1=1,\rho_4=-2$ in (16) yields the following

$$\mathscr{Q}_{1,2}(x,t)=\frac{4\cosh\left(-2+\frac{(512t+4x)\sqrt{510}}{255}\right)+4\sinh\left(-2+\frac{(512t+4x)\sqrt{510}}{255}\right)-16\cosh\left(2+\frac{(512t+4x)\sqrt{510}}{255}\right)+16\sinh\left(2+\frac{(512t+4x)\sqrt{510}}{255}\right)}{\cosh\left(-2+\frac{(512t+4x)\sqrt{510}}{255}\right)+\sinh\left(-2+\frac{(512t+4x)\sqrt{510}}{255}\right)+4\cosh\left(2+\frac{(512t+4x)\sqrt{510}}{255}\right)-4\sinh\left(2+\frac{(512t+4x)\sqrt{510}}{255}\right)}\times e^{i\Phi}, \tag{13}$$

Box III.

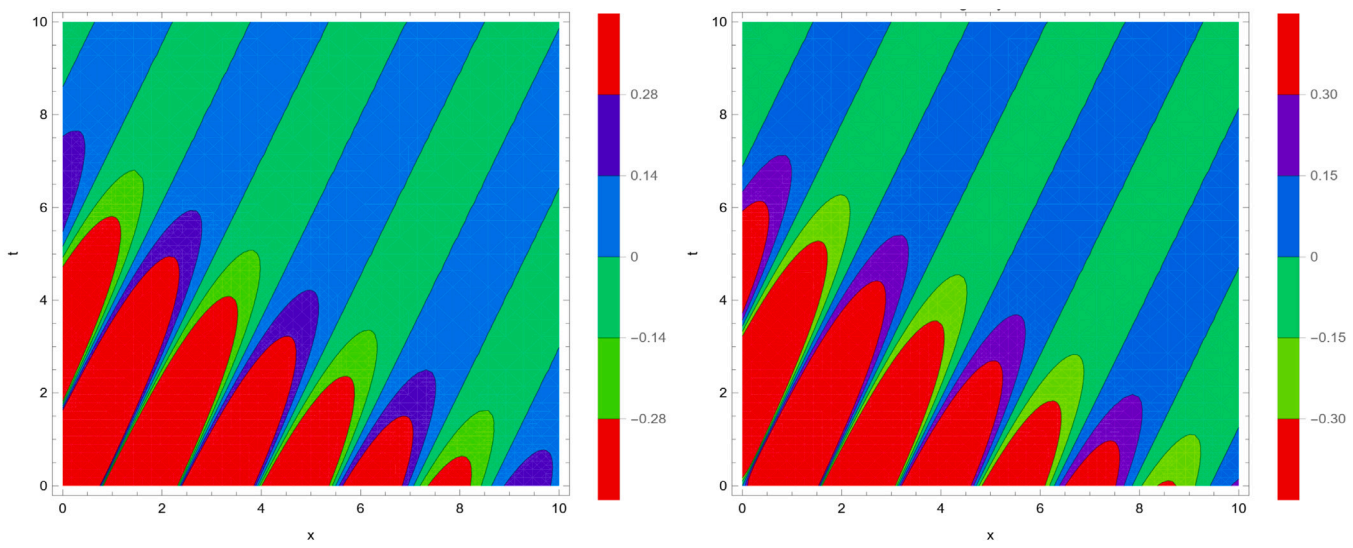

Fig. 1. The wave solution $\mathscr{Q}_1(x,t)$ given by (10). **Left:** Real part, **Right:** Imaginary part.

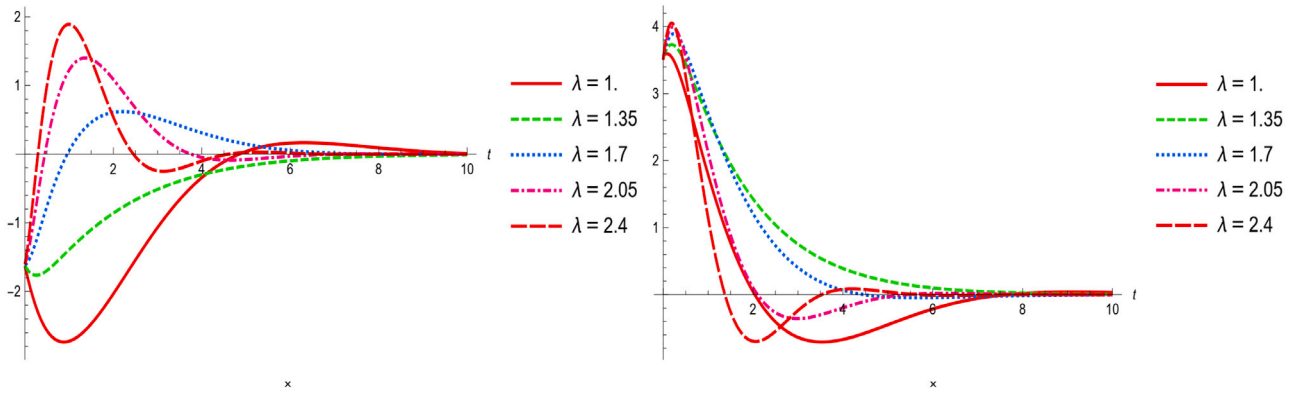

Fig. 2. The effects of λ on $\mathscr{Q}_1(x=0.48,t)$ given by (10) for $\gamma=2.94$. **Left:** Real part, **Right:** Imaginary part.

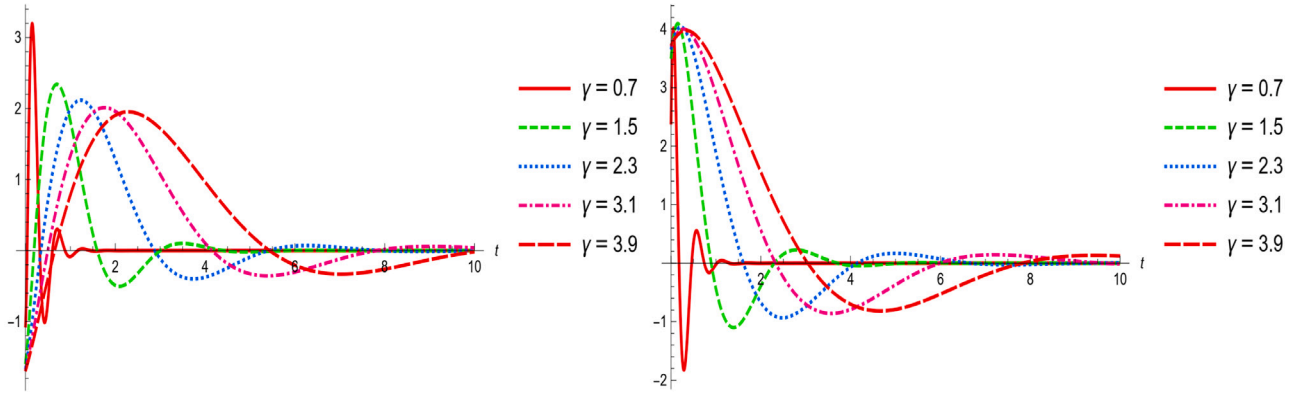

Fig. 3. The effects of γ on $\mathscr{Q}_1(x=0.48,t)$ given by (10) for $\lambda=0.4$. **Left:** Real part, **Right:** Imaginary part.

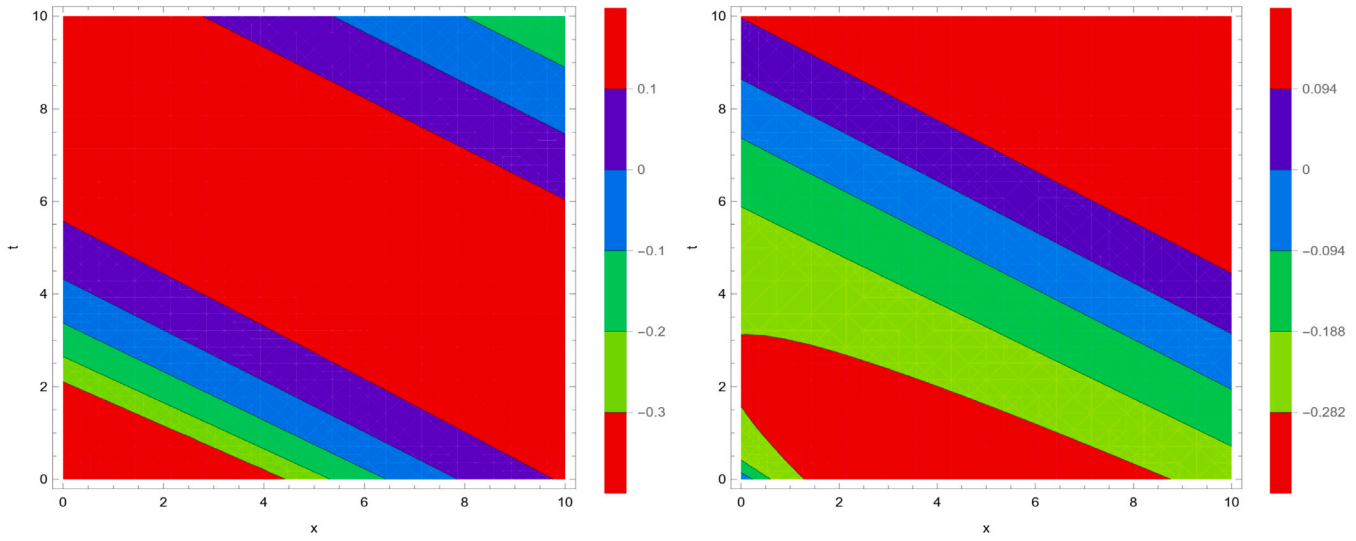

Fig. 4. The wave solution $\mathscr{Q}_2(x,t)$ given by (16). **Left:** Real part, **Right:** Imaginary part.

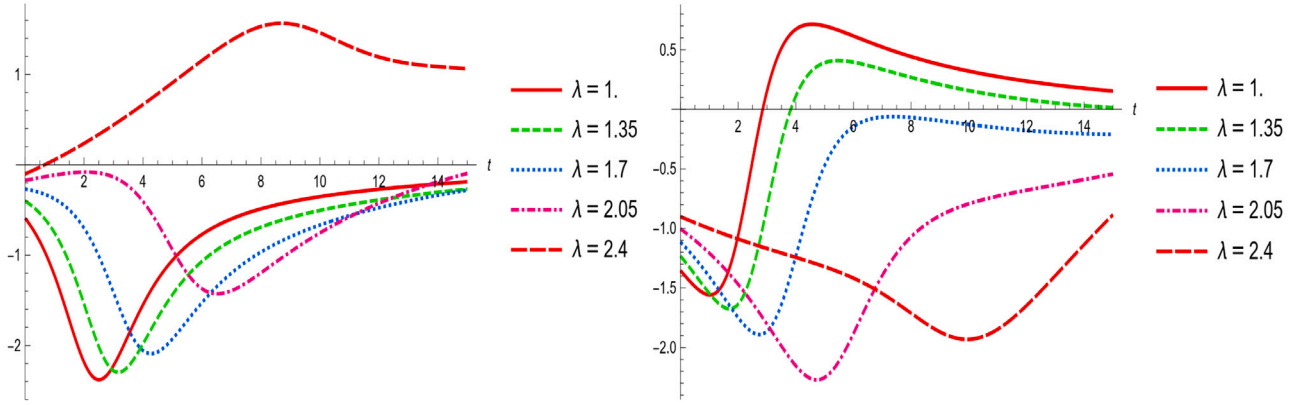

Fig. 5. The effects of λ on $\mathscr{Q}_2(x=0.48,t)$ given by (16) for $\gamma=2.94$. **Left:** Real part, **Right:** Imaginary part.

analytical solution

$$\mathscr{Q}_{2,2}(x,t) = \frac{-4\sinh\left(\frac{(80t+36x)\sqrt{31}}{93}\right)+4\cosh\left(\frac{(80t+36x)\sqrt{31}}{93}\right)-2}{2\sinh\left(\frac{(80t+36x)\sqrt{31}}{93}\right)-2\cosh\left(\frac{(80t+36x)\sqrt{31}}{93}\right)-1} \times e^{i\left(-\frac{4t}{3}+2x\right)}. \tag{19}$$

In Fig. 4, we have demonstrated corresponding dynamic behavior related to the analytical solution obtained in (16) for $\alpha_1 = 0.48, \alpha_4 = 0.48, \beta_1 = 0.48, \beta_4 = 0.48, \rho_1 = 0.48, \rho_4 = 0.7$, and $\sigma = 0.2, \lambda = 2, \gamma = 3.35$. In addition, the sensitivity of this solution is demonstrated based on the changes of two parameters λ and γ in Figs. 5 and 6, respectively. In these diagrams, the instability of the behavior of the solutions for some values of the parameters is clearly observed.

Category 3: In this case, we obtain

$$\kappa = \frac{2\sqrt{\left(8\gamma^2\lambda\alpha_2^2-16\gamma^2\lambda\alpha_2\alpha_3+8\gamma^2\lambda\alpha_3^2-1\right)\lambda(\gamma\sigma-1)}}{8\gamma^2\lambda\alpha_2^2-16\gamma^2\lambda\alpha_2\alpha_3+8\gamma^2\lambda\alpha_3^2-1}, \mu = -\frac{8\lambda\alpha_2^2-16\alpha_3\lambda\alpha_2+8\alpha_3^2\lambda-\sigma^2}{\gamma\sigma-1},$$
$$\sigma=\sigma, \alpha_1=\alpha_1, \alpha_2=\alpha_2, \alpha_3=\alpha_3, \alpha_4=\alpha_4,$$
$$\beta_1=\beta_1, \beta_2=\beta_2, \beta_3=\beta_3, \beta_4=\beta_4, \rho_0=0, \rho_1=0, \rho_2=\rho_2, \rho_3=\rho_3, \rho_4=0. \tag{20}$$

Inserting these values into Eq. (7) yields

$$\mathrm{q}(\zeta) = \frac{\rho_2 e^{\zeta\alpha_2+\beta_2}}{\rho_3 e^{\zeta\alpha_3+\beta_3}} + \frac{\rho_3 e^{\zeta\alpha_3+\beta_3}}{\rho_2 e^{\zeta\alpha_2+\beta_2}}. \tag{21}$$

Hence we conclude

$$\mathscr{Q}(\zeta) = \frac{2(\alpha_2-\alpha_3)\left(\rho_2 e^{\zeta\alpha_2+\beta_2}-\rho_3 e^{\zeta\alpha_3+\beta_3}\right)\left(\rho_2 e^{\zeta\alpha_2+\beta_2}+\rho_3 e^{\zeta\alpha_3+\beta_3}\right)}{\left(e^{\zeta\alpha_2+\beta_2}\right)^2\rho_2^2+\rho_3^2\left(e^{\zeta\alpha_3+\beta_3}\right)^2}.$$

Accordingly, the analytical solution in this case, is structured as follows

$$\mathscr{Q}_3(x,t) = \frac{2(\alpha_2-\alpha_3)\left(\rho_2 e^{\zeta\alpha_2+\beta_2}-\rho_3 e^{\zeta\alpha_3+\beta_3}\right)\left(\rho_2 e^{\zeta\alpha_2+\beta_2}+\rho_3 e^{\zeta\alpha_3+\beta_3}\right)}{\left(e^{\zeta\alpha_2+\beta_2}\right)^2\rho_2^2+\rho_3^2\left(e^{\zeta\alpha_3+\beta_3}\right)^2} \times e^{i\boldsymbol{\Phi}(x,t)}, \tag{22}$$

where

$$\zeta = \frac{\sqrt{8}\sqrt{\lambda\left(-\frac{1}{8}+\gamma^2(\alpha_2-\alpha_3)^2\lambda\right)}\left(\gamma^2\sigma^2x+\left(8t(\alpha_2-\alpha_3)^2\lambda+\sigma^2t-2\sigma x\right)\gamma-2\sigma t+x\right)}{4(\gamma\sigma-1)\left(-\frac{1}{8}+\gamma^2(\alpha_2-\alpha_3)^2\lambda\right)},$$
$$\boldsymbol{\Phi} = -\frac{\left(8\lambda\alpha_2^2-16\alpha_3\lambda\alpha_2+8\alpha_3^2\lambda-\sigma^2\right)t}{\gamma\sigma-1}+\sigma x. \tag{23}$$

Further, solution (22) covers abundant analytical solutions for the main equation, which are described below.

Sub-family 1: Considering the case of $\gamma=2, \lambda=1, \sigma=2, \alpha_2=\mathrm{i}, \alpha_3=-1+\mathrm{i}, \beta_2=-\mathrm{i}, \beta_3=-\mathrm{i}, \rho_2=1, \rho_3=-\mathrm{i}$ in (22) yields the following analytical solution

$$\mathscr{Q}_{3,1}(x,t) = \frac{-2\sinh\left(\frac{(80t+36x)\sqrt{31}}{93}\right)+2\cosh\left(\frac{(80t+36x)\sqrt{31}}{93}\right)+2}{\sinh\left(\frac{(80t+36x)\sqrt{31}}{93}\right)-\cosh\left(\frac{(80t+36x)\sqrt{31}}{93}\right)+1} \times e^{i\left(-\frac{4t}{3}+2x\right)}. \tag{24}$$

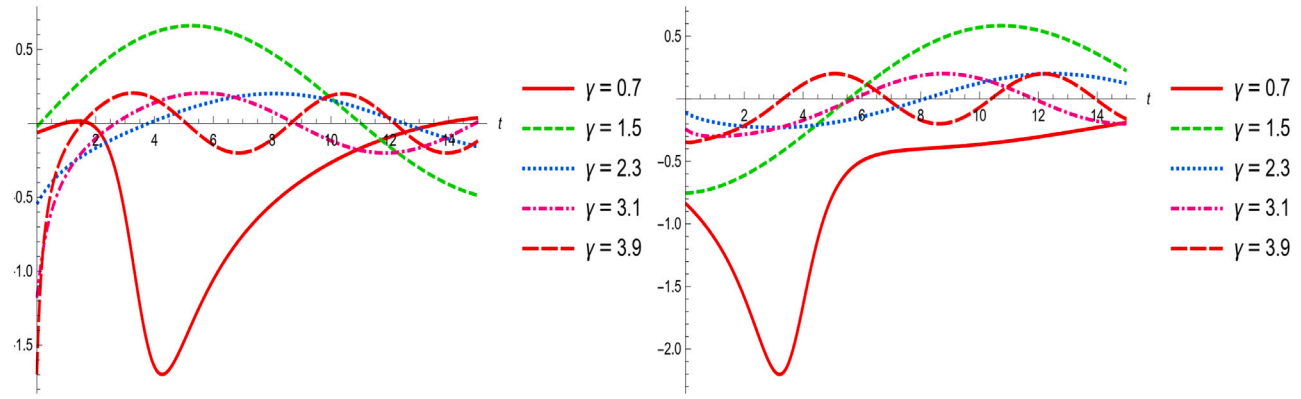

Fig. 6. The effects of γ on $\mathscr{Q}_2(x=0.48,t)$ given by (16) for $\lambda=0.6$. **Left:** Real part, **Right:** Imaginary part.

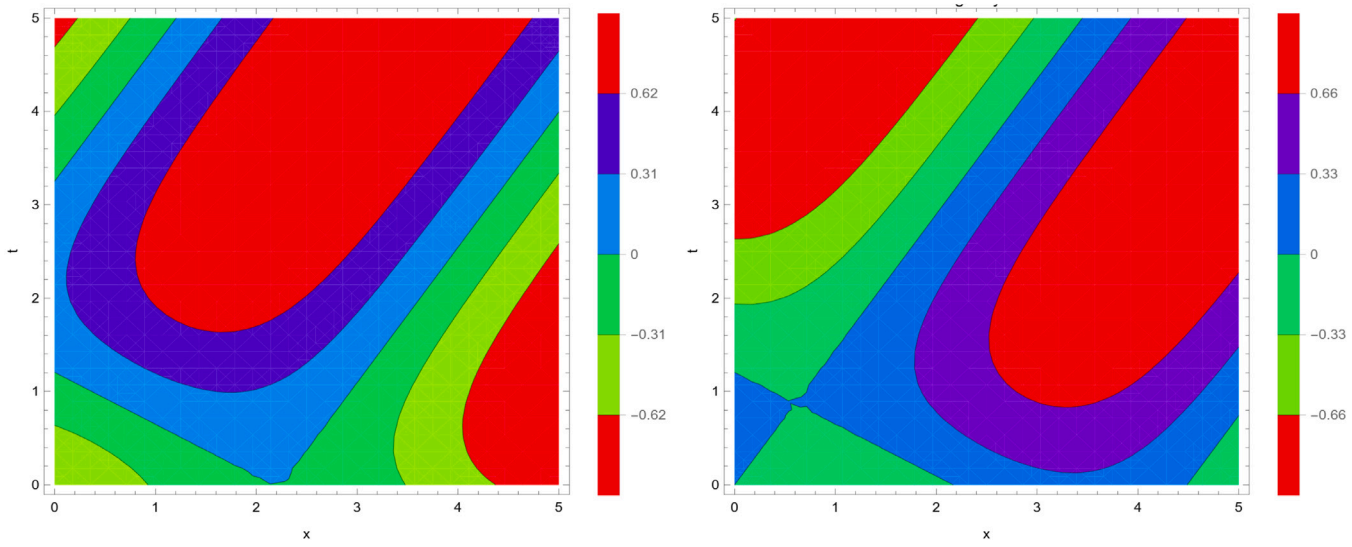

Fig. 7. The wave solution $\mathscr{Q}_3(x,t)$ given by (22). **Left:** Real part, **Right:** Imaginary part.

Sub-family 2: Considering the case of $\gamma=2,\lambda=1,\sigma=2,\alpha_2=1,\alpha_3=-1,\beta_2=-\mathrm{i},\beta_3=-\mathrm{i},\rho_2=1,\rho_3=-\mathrm{i}$ in (22) yields the following analytical solution

$$\mathscr{Q}_{3,2}(x,t)=\frac{4+4\cosh\left(\frac{(72x+544t)\sqrt{127}}{381}\right)+4\sinh\left(\frac{(72x+544t)\sqrt{127}}{381}\right)}{-1+\cosh\left(\frac{(72x+544t)\sqrt{127}}{381}\right)+\sinh\left(\frac{(72x+544t)\sqrt{127}}{381}\right)}\times \mathrm{e}^{\mathrm{i}\left(-\frac{28t}{3}+2x\right)}. \tag{25}$$

In Fig. 7, we have demonstrated corresponding dynamic behavior related to the analytical solution obtained in (22) for $\alpha_2=0.1,\alpha_3=0.1,\beta_2=0.2,\beta_3=0.48,\rho_2=0.48,\rho_3=0.2$, and $\sigma=0.7,\lambda=0.7,\gamma=4.12$. In addition, the sensitivity of this solution is demonstrated based on the changes of two parameters λ and γ in Figs. 8 and 9, respectively. In these plots, we observe the effects of considered parameters on the behavior of the solutions.

Category 4: In this case, we obtain

$$\kappa=\frac{4\sqrt{\left(8\gamma^2\lambda\alpha_2^2-16\gamma^2\lambda\alpha_2\alpha_4+8\gamma^2\lambda\alpha_4^2-1\right)\lambda(\gamma\sigma-1)}}{8\gamma^2\lambda\alpha_2^2-16\gamma^2\lambda\alpha_2\alpha_4+8\gamma^2\lambda\alpha_4^2-1},\ \mu=-\frac{8\lambda\alpha_2^2-16\alpha_4\lambda\alpha_2+8\alpha_4^2\lambda-\sigma^2}{\gamma\sigma-1},$$
$$\sigma=\sigma,\alpha_1=\alpha_1,\alpha_2=\alpha_2,\alpha_3=\alpha_4,\alpha_4=\alpha_4,$$
$$\beta_1=\beta_1,\beta_2=\beta_2,\beta_3=\beta_3,\beta_4=\beta_4,\rho_0=-2,\rho_1=0,\rho_2=\rho_2,\rho_3=\rho_3,\rho_4=\rho_4. \tag{26}$$

Inserting these values into Eq. (7) yields

$$\mathrm{q}(\zeta)=\frac{\left(\rho_2\mathrm{e}^{\zeta\alpha_2+\beta_2}-\rho_3\mathrm{e}^{\zeta\alpha_4+\beta_3}-\rho_4\mathrm{e}^{\zeta\alpha_4+\beta_4}\right)^2}{\left(\rho_3\mathrm{e}^{\zeta\alpha_4+\beta_3}+\rho_4\mathrm{e}^{\zeta\alpha_4+\beta_4}\right)\rho_2\mathrm{e}^{\zeta\alpha_2+\beta_2}}. \tag{27}$$

So, we get

$$\mathscr{Q}(\zeta)=\frac{2(\alpha_2-\alpha_4)\left(\rho_2\mathrm{e}^{\zeta\alpha_2+\beta_2}+\rho_3\mathrm{e}^{\zeta\alpha_4+\beta_3}+\rho_4\mathrm{e}^{\zeta\alpha_4+\beta_4}\right)}{\rho_2\mathrm{e}^{\zeta\alpha_2+\beta_2}-\rho_3\mathrm{e}^{\zeta\alpha_4+\beta_3}-\rho_4\mathrm{e}^{\zeta\alpha_4+\beta_4}}.$$

Hence, the analytical solution in this case, is structured as follows

$$\mathscr{Q}_4(x,t)=\frac{2(\alpha_2-\alpha_4)\left(\rho_2\mathrm{e}^{\zeta\alpha_2+\beta_2}+\rho_3\mathrm{e}^{\zeta\alpha_4+\beta_3}+\rho_4\mathrm{e}^{\zeta\alpha_4+\beta_4}\right)}{\rho_2\mathrm{e}^{\zeta\alpha_2+\beta_2}-\rho_3\mathrm{e}^{\zeta\alpha_4+\beta_3}-\rho_4\mathrm{e}^{\zeta\alpha_4+\beta_4}}\times e^{i\Phi(x,t)}, \tag{28}$$

where

$$\zeta=\frac{\sqrt{8}\sqrt{\lambda\left(-\frac{1}{8}+\gamma^2(\alpha_2-\alpha_4)^2\lambda\right)}\left(\gamma^2\sigma^2x+\left(8t(\alpha_2-\alpha_4)^2\lambda+\sigma^2t-2\sigma x\right)\gamma-2\sigma t+x\right)}{2(\gamma\sigma-1)\left(-\frac{1}{8}+\gamma^2(\alpha_2-\alpha_4)^2\lambda\right)},$$
$$\Phi=-\frac{\left(8\lambda\alpha_2^2-16\alpha_4\lambda\alpha_2+8\alpha_4^2\lambda-\sigma^2\right)t}{\gamma\sigma-1}+\sigma x. \tag{29}$$

It should be noted that solution (28) covers abundant analytical solutions for the main equation. Some of the special cases for this category of solutions are listed below.

Sub-family 1: Considering the case of $\gamma=2,\lambda=1,\sigma=2,\alpha_2=2,\alpha_4=-1,\beta_2=1,\beta_3=-1,\beta_4=1,\rho_2=1,\rho_3=1,\rho_4=0$ in (28) yields the following analytical solution

$$\mathscr{Q}_{4,1}(x,t)=\frac{6\cosh(\zeta)+6\sinh(\zeta)+6\cosh(\zeta)-6\sinh(\zeta)}{\cosh(\zeta)+\sinh(\zeta)-\cosh(\zeta)+\sinh(\zeta)}\times\mathrm{e}^{\mathrm{i}\Phi}. \tag{30}$$

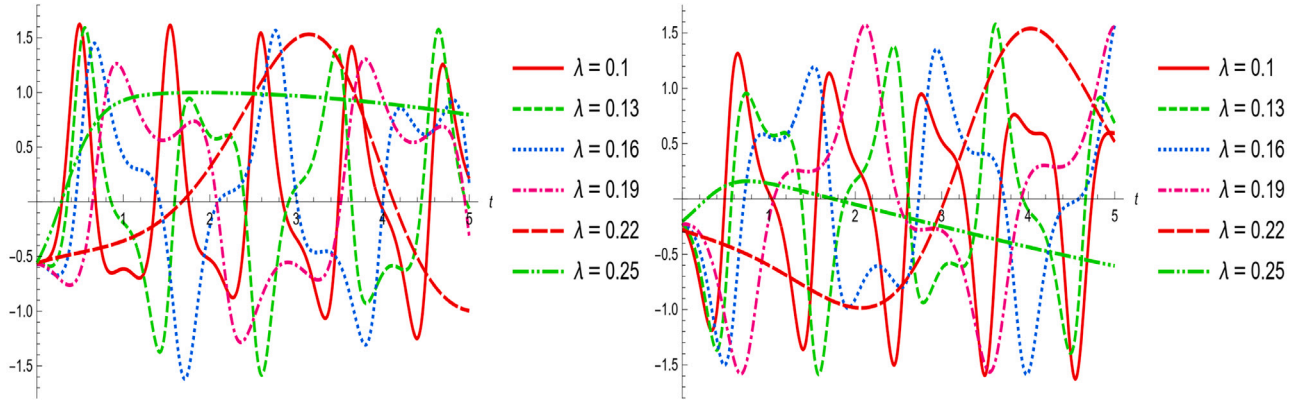

Fig. 8. The effects of λ on $\mathscr{Q}_3(x=0.48,t)$ given by (22) for $\gamma=2.94$. **Left:** Real part, **Right:** Imaginary part.

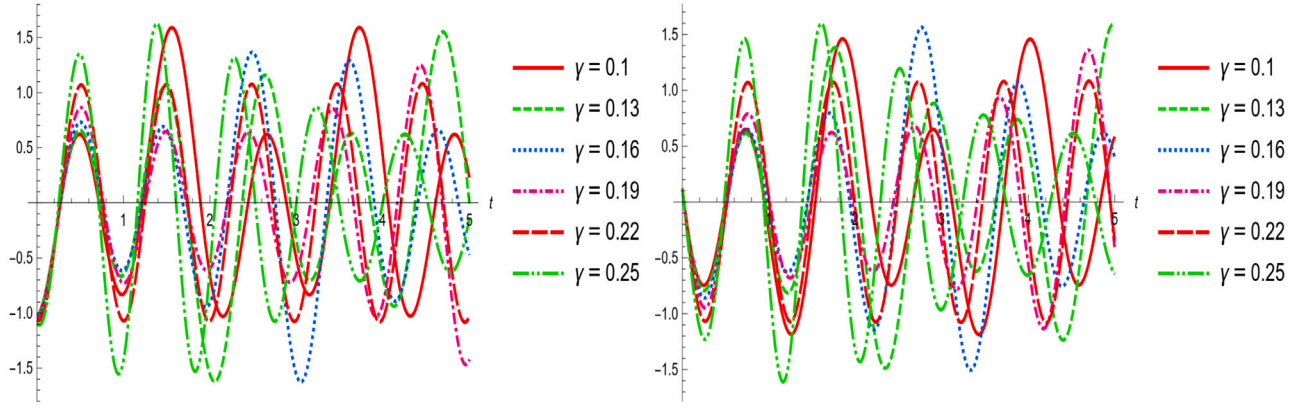

Fig. 9. The effects of γ on $\mathscr{Q}_3(x=0.48,t)$ given by (22) for $\lambda=0.7$. **Left:** Real part, **Right:** Imaginary part.

where $\zeta=0.48+\frac{(592t+36x)\sqrt{287}}{861}, \Phi=-\frac{68t}{3}+2x$.

Sub-family 2: Considering the case of $\gamma=-1,\lambda=2,\sigma=1,\alpha_2=-1+\mathrm{i},\alpha_4=\mathrm{i},\beta_2=1,\beta_3=-1,\beta_4=1,\rho_2=\mathrm{i},\rho_3=\mathrm{i},\rho_4=-\mathrm{i}$ in (28) yields the following analytical solution

$$\mathscr{Q}_{4,2}(x,t)=\frac{-2-2\cosh(-2+2\zeta)+2\sinh(-2+2\zeta)+2\cosh(2)+2\sinh(2)}{-1+\cosh(-2+2\zeta)-\sinh(-2+2\zeta)+\cosh(2)+\sinh(2)}\times e^{\mathrm{i}\left(\frac{15t}{2}+x\right)}. \tag{31}$$

In Fig. 10, we have demonstrated corresponding dynamic behavior related to the analytical solution obtained in (28) for $\alpha_2=0.1,\alpha_3=0.48,\alpha_4=0.48,\beta_2=0.2,\beta_3=0.48,\beta_4=0.48,\rho_2=0.48,\rho_3=0.2,\rho_4=0.2$, and $\sigma=0.1,\lambda=0.48,\gamma=3$. In addition, the sensitivity of this solution is demonstrated based on the changes of two parameters λ and γ in Figs. 11 and 12, respectively. In these diagrams, it can be seen that increasing the value of the parameters will make the solutions more stable in the considered conditions.

Category 5: In this case, we obtain

$$\kappa=\frac{2\sqrt{\left(8\gamma^2\lambda\alpha_2^2-16\gamma^2\lambda\alpha_2\alpha_3+8\gamma^2\lambda\alpha_3^2-1\right)\lambda(\gamma\sigma-1)}}{8\gamma^2\lambda\alpha_2^2-16\gamma^2\lambda\alpha_2\alpha_3+8\gamma^2\lambda\alpha_3^2-1},\ \mu=-\frac{8\lambda\alpha_2^2-16\alpha_3\lambda\alpha_2+8\alpha_3^2\lambda-\sigma^2}{\gamma\sigma-1},$$
$$\sigma=\sigma,\alpha_1=\alpha_2,\alpha_2=\alpha_2,\alpha_3=\alpha_3,\alpha_4=\alpha_4,$$
$$\beta_1=\beta_1,\beta_2=\beta_2,\beta_3=\beta_3,\beta_4=\beta_4,\rho_0=0,\rho_1=\rho_1,\rho_2=\rho_2,\rho_3=\rho_3,\rho_4=0. \tag{32}$$

Inserting these values into Eq. (7) yields

$$\mathrm{q}(\zeta)=\frac{\rho_1 e^{\zeta\alpha_2+\beta_1}+\rho_2 e^{\zeta\alpha_2+\beta_2}}{\rho_3 e^{\zeta\alpha_3+\beta_3}}+\frac{\rho_3 e^{\zeta\alpha_3+\beta_3}}{\rho_1 e^{\zeta\alpha_2+\beta_1}+\rho_2 e^{\zeta\alpha_2+\beta_2}}. \tag{33}$$

Hence we conclude

$$\mathscr{Q}(\zeta)=\frac{2(\alpha_2-\alpha_3)\left(\rho_1 e^{\zeta\alpha_2+\beta_1}+\rho_2 e^{\zeta\alpha_2+\beta_2}-\rho_3 e^{\zeta\alpha_3+\beta_3}\right)\left(\rho_1 e^{\zeta\alpha_2+\beta_1}+\rho_2 e^{\zeta\alpha_2+\beta_2}+\rho_3 e^{\zeta\alpha_3+\beta_3}\right)}{\left(e^{\zeta\alpha_2+\beta_1}\right)^2\rho_1^2+2e^{\zeta\alpha_2+\beta_1}e^{\zeta\alpha_2+\beta_2}\rho_1\rho_2+\left(e^{\zeta\alpha_2+\beta_2}\right)^2\rho_2^2+\rho_3^2\left(e^{\zeta\alpha_3+\beta_3}\right)^2}.$$

Therefore, the analytical solution in this case, is structured as follows (see Eq. (34) given as in Box IV)
where

$$\zeta=\frac{\sqrt{8}\sqrt{\lambda\left(-\frac{1}{8}+\gamma^2(\alpha_2-\alpha_3)^2\lambda\right)}\left(\gamma^2\sigma^2x+\left(8t(\alpha_2-\alpha_3)^2\lambda+\sigma^2t-2\sigma x\right)\gamma-2\sigma t+x\right)}{4(\gamma\sigma-1)\left(-\frac{1}{8}+\gamma^2(\alpha_2-\alpha_3)^2\lambda\right)},$$
$$\Phi=-\frac{\left(8\lambda\alpha_2^2-16\alpha_3\lambda\alpha_2+8\alpha_3^2\lambda-\sigma^2\right)t}{\gamma\sigma-1}+\sigma x. \tag{35}$$

The general solution obtained in Eq. (34) contains abundant analytical solutions for the main equation. Some of them can be expressed as follows.

Sub-family 1: Considering the case of $\gamma=-1,\lambda=2,\sigma=1,\alpha_2=1+\mathrm{i},\alpha_3=\mathrm{i},\beta_1=1,\beta_2=-1,\beta_3=1,\rho_1=\mathrm{i},\rho_2=\mathrm{i},\rho_3=-\mathrm{i}$ in (34) yields the following analytical solution (see Eq. (36) given as in Box V)

where $\zeta=\frac{\sqrt{30}(19t-4x)}{15}, \Phi=\frac{15t}{2}+x$.

Sub-family 2: Considering the case of $\gamma=-1,\lambda=2,\sigma=1,\alpha_2=1+\mathrm{i},\alpha_3=\mathrm{i},\beta_1=1,\beta_2=-1,\beta_3=1,\rho_1=-1,\rho_2=1,\rho_3=1$ in (34) yields the following analytical solution (see Eq. (37) given as in Box VI)

where $\zeta=\frac{\sqrt{30}(19t-4x)}{15}, \Phi=\frac{15t}{2}+x$.

In order to investigate the dynamic behavior related to the analytical solution obtained in Eq. (34), we plot the solution through taking $\alpha_2=0.48,\alpha_3=0.2,\beta_1=0.48,\beta_2=0.48,\rho_1=0.8,\rho_2=\rho_4=0.48$, and $\sigma=0.48.8,\lambda=0.95,\gamma=7.94$ in Fig. 13. In addition, the sensitivity of this solution is demonstrated based on the changes of two parameters λ and γ in Figs. 14 and 15, respectively. In each case, the changes associated

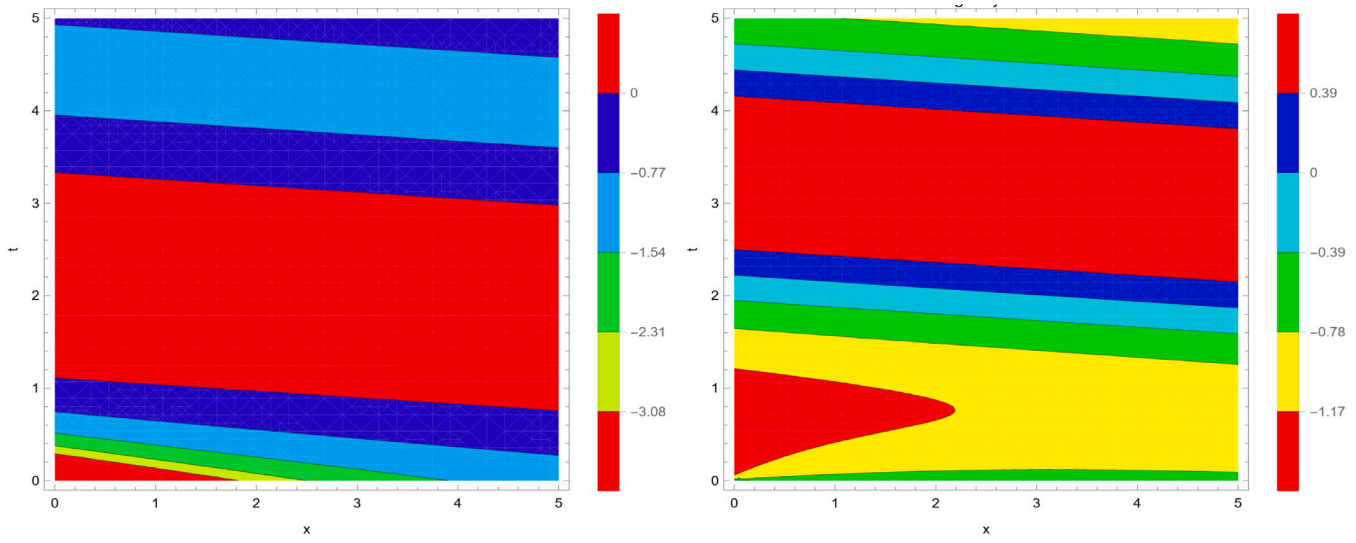

Fig. 10. The wave solution $\mathscr{Q}_4(x,t)$ given by (28). **Left:** Real part, **Right:** Imaginary part.

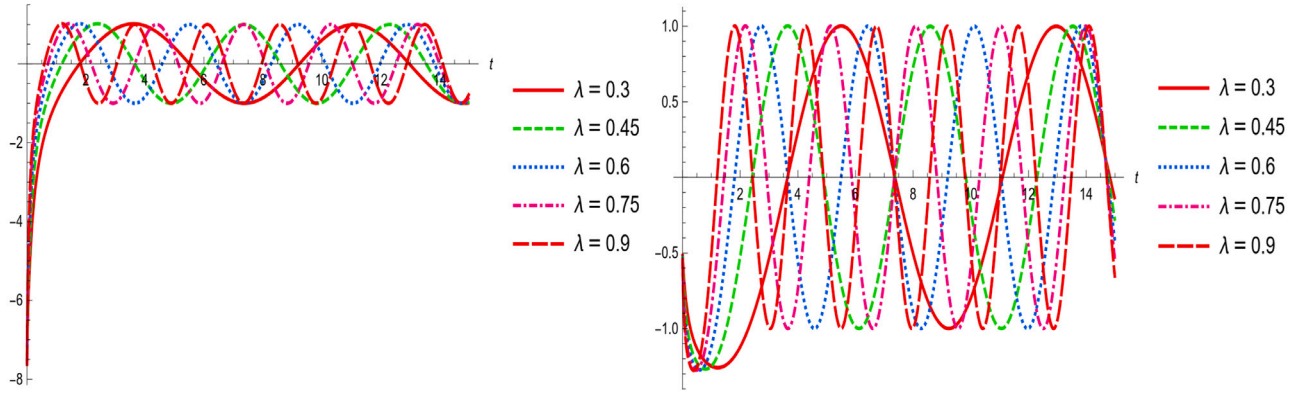

Fig. 11. The effects of λ on $\mathscr{Q}_4(x=0.7,t)$ given by (28) for $\gamma=0.5$. **Left:** Real part, **Right:** Imaginary part.

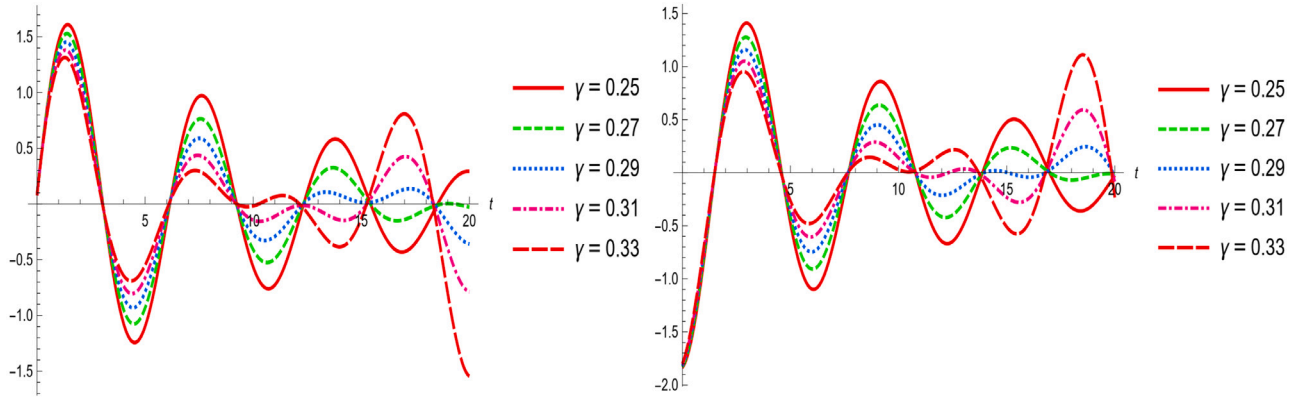

Fig. 12. The effects of γ on $\mathscr{Q}_4(x=0.7,t)$ given by (28) for $\lambda=0.6$. **Left:** Real part, **Right:** Imaginary part.

$$\mathscr{Q}_5(x,t)=\frac{2\left(\alpha_2-\alpha_3\right)\left(\rho_1 e^{\zeta\alpha_2+\beta_1}+\rho_2 e^{\zeta\alpha_2+\beta_2}-\rho_3 e^{\zeta\alpha_3+\beta_3}\right)\left(\rho_1 e^{\zeta\alpha_2+\beta_1}+\rho_2 e^{\zeta\alpha_2+\beta_2}+\rho_3 e^{\zeta\alpha_3+\beta_3}\right)}{\left(e^{\zeta\alpha_2+\beta_1}\right)^2\rho_1^2+2\,e^{\zeta\alpha_2+\beta_1}e^{\zeta\alpha_2+\beta_2}\rho_1\rho_2+\left(e^{\zeta\alpha_2+\beta_2}\right)^2\rho_2^2+\rho_3^2\left(e^{\zeta\alpha_3+\beta_3}\right)^2}\times e^{i\Phi(x,t)}, \tag{34}$$

Box IV.

$$\mathscr{Q}_{5,1}(x,t)=\frac{16\left(\cosh^2(\zeta)\right)\left(\cosh^2(1)\right)+8\sinh(2\zeta)\left(\cosh^2(1)\right)-12\left(\cosh^2(1)\right)-4\cosh(1)\sinh(1)+2}{2\cosh(2)\sinh(2\zeta)+2\sinh(2\zeta)+2\cosh(2)\cosh(2\zeta)+2\cosh(2\zeta)+\sinh(2)+\cosh(2)}\times e^{i\Phi}, \tag{36}$$

Box V.

$$\mathscr{Q}_{5,2}(x,t)=\frac{\left(16\cosh^2(\zeta)\left(\cosh^2(1)\right)-16\right)+\left(8\sinh(2\zeta)\left(\cosh^2(1)\right)-16\right)-12\left(\cosh^2(1)\right)-2\sinh(2)+10}{2\cosh(2)\cosh(2\zeta)+2\cosh(2)\sinh(2\zeta)-2\cosh(2\zeta)-2\sinh(2\zeta)+\cosh(2)+\sinh(2)}\times e^{i\Phi}, \tag{37}$$

Box VI.

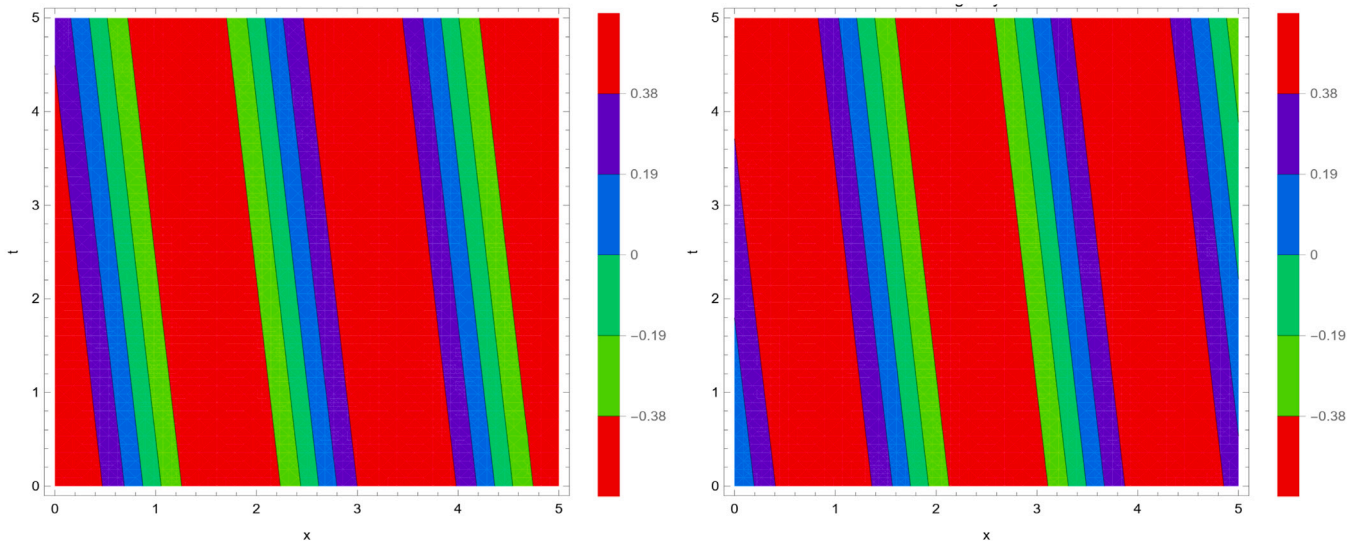

Fig. 13. The wave solution $\mathscr{Q}_5(x,t)$ given by (34). **Left:** Real part, **Right:** Imaginary part.

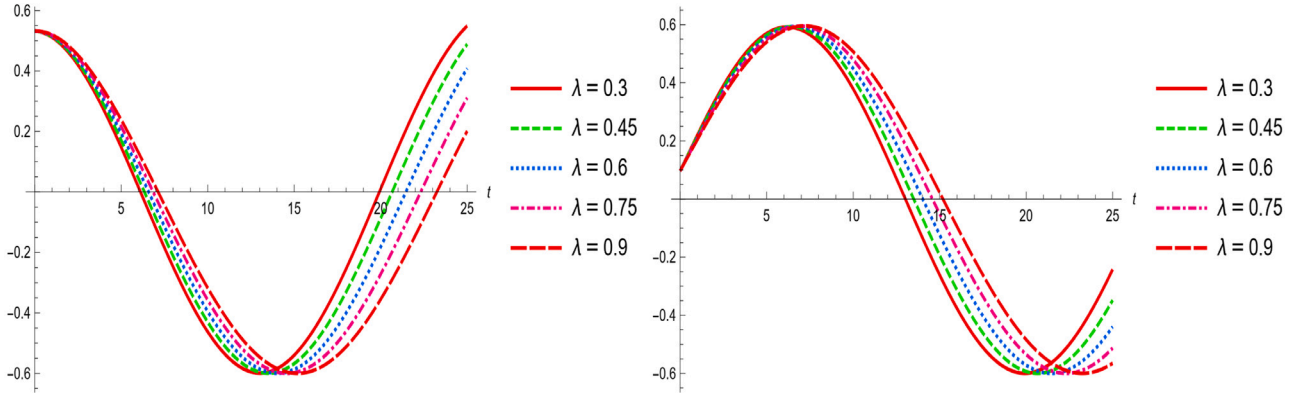

Fig. 14. The effects of λ on $\mathscr{Q}_5(x=0.1,t)$ given by (34) for $\gamma=0.95$. **Left:** Real part, **Right:** Imaginary part.

with each parameter clearly reveal significant effects on the solution behavior of the equation.

Category 6: In this case, the following values are solutions are determined

$$\kappa=\frac{2\sqrt{\left(8\gamma^2\lambda\alpha_1^2-16\gamma^2\lambda\alpha_1\alpha_4+8\gamma^2\lambda\alpha_4^2-1\right)\lambda(\gamma\sigma-1)}}{8\gamma^2\lambda\alpha_1^2-16\gamma^2\lambda\alpha_1\alpha_4+8\gamma^2\lambda\alpha_4^2-1},\ \mu=-\frac{8\lambda\alpha_1^2-16\alpha_4\lambda\alpha_1+8\alpha_4^2\lambda-\sigma^2}{\gamma\sigma-1},$$
$$\sigma=\sigma,\alpha_1=\alpha_1,\alpha_2=\alpha_2,\alpha_3=\alpha_3,\alpha_4=\alpha_4,$$
$$\beta_1=\beta_1,\beta_2=\beta_2,\beta_3=\beta_3,\beta_4=\beta_4,\rho_0=0,\rho_1=\rho_1,\rho_2=0,\rho_3=0,\rho_4=\rho_4. \tag{38}$$

Inserting these values into Eq. (7) yields

$$q(\zeta)=\frac{\rho_1 e^{\zeta\alpha_1+\beta_1}}{\rho_4 e^{\zeta\alpha_4+\beta_4}}+\frac{\rho_4 e^{\zeta\alpha_4+\beta_4}}{\rho_1 e^{\zeta\alpha_1+\beta_1}}. \tag{39}$$

So, we get

$$\mathscr{Q}(\zeta)=-\frac{2\left(\alpha_1-\alpha_4\right)\left(\rho_4 e^{\zeta\alpha_4+\beta_4}-\rho_1 e^{\zeta\alpha_1+\beta_1}\right)\left(\rho_1 e^{\zeta\alpha_1+\beta_1}+\rho_4 e^{\zeta\alpha_4+\beta_4}\right)}{\rho_1^2\left(e^{\zeta\alpha_1+\beta_1}\right)^2+\rho_4^2\left(e^{\zeta\alpha_4+\beta_4}\right)^2}.$$

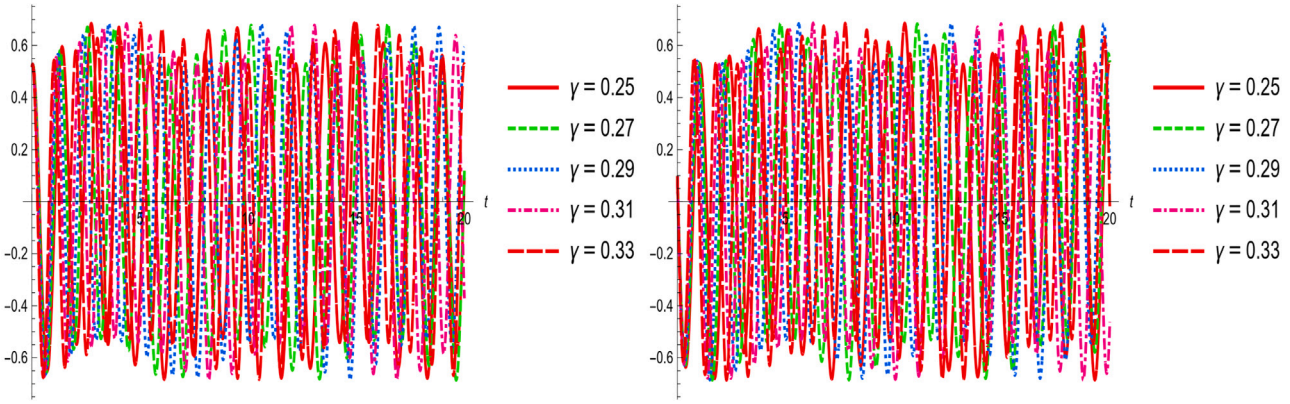

Fig. 15. The effects of γ on $\mathscr{Q}_5\,(x=0.1,t)$ given by (34) for $\lambda=1.2$. **Left:** Real part, **Right:** Imaginary part.

$$\mathscr{Q}_{6,2}\,(x,t)=\frac{24\cosh\left(-2+\frac{(294t-8x)\sqrt{286}}{143}\right)+24\sinh\left(-2+\frac{(294t-8x)\sqrt{286}}{143}\right)+6\cosh\left(4+\frac{(588t-16x)\sqrt{286}}{143}\right)-6\sinh\left(4+\frac{(588t-16x)\sqrt{286}}{143}\right)}{4\cosh\left(-2+\frac{(294t-8x)\sqrt{286}}{143}\right)+4\sinh\left(-2+\frac{(294t-8x)\sqrt{286}}{143}\right)-\cosh\left(4+\frac{(588t-16x)\sqrt{286}}{143}\right)+\sinh\left(4+\frac{(588t-16x)\sqrt{286}}{143}\right)}\times e^{\Phi},\tag{43}$$

Box VII.

Accordingly, the analytical solution in this case, is structured as follows

$$\mathscr{Q}_6\,(x,t)=-\frac{2\left(\alpha_1-\alpha_4\right)\left(\rho_4e^{\zeta\alpha_4+\beta_4}-\rho_1e^{\zeta\alpha_1+\beta_1}\right)\left(\rho_1e^{\zeta\alpha_1+\beta_1}+\rho_4e^{\zeta\alpha_4+\beta_4}\right)}{\rho_1^2\left(e^{\zeta\alpha_1+\beta_1}\right)^2+\rho_4^2\left(e^{\zeta\alpha_4+\beta_4}\right)^2}\times e^{i\Phi(x,t)},\tag{40}$$

where

$$\zeta=\frac{\sqrt{8}\sqrt{\lambda\left(-\frac{1}{8}+\gamma^2(\alpha_1-\alpha_4)^2\lambda\right)}\left(\gamma^2\sigma^2x+\left(8t(\alpha_1-\alpha_4)^2\lambda+\sigma^2t-2\sigma x\right)\gamma-2\sigma t+x\right)}{4(\gamma\sigma-1)\left(-\frac{1}{8}+\gamma^2(\alpha_1-\alpha_4)^2\lambda\right)},$$
$$\Phi=-\frac{\left(8\lambda\alpha_1^2-16\alpha_4\lambda\alpha_1+8\alpha_4^2\lambda-\sigma^2\right)t}{\gamma\sigma-1}+\sigma x.\tag{41}$$

Further, solution (40) covers abundant analytical solutions for the main equation, which are described below.

Sub-family 1: Considering the case of $\gamma=-1,\lambda=2,\sigma=1,\alpha_1=\mathrm{I},\alpha_4=1+\mathrm{I},\beta_1=1,\beta_4=-1,\rho_1=-1,\rho_4=1$ in (40) yields the following analytical solution

$$\mathscr{Q}_{6,1}\,(x,t)=\frac{-2\cosh(2)-2\sinh(2)+2\cosh(-2+2\zeta)+2\sinh(-2+2\zeta)}{\cosh(2)+\sinh(2)+\cosh(-2+2\zeta)+\sinh(-2+2\zeta)}\times e^{\mathrm{I}\left(\frac{15t}{2}+x\right)}.\tag{42}$$

where $\Phi=-\frac{68t}{3}+2x$.

Sub-family 2: Considering the case of $\gamma=-1,\lambda=2,\sigma=1,\alpha_1=1,\alpha_4=-2,\beta_1=-1,\beta_4=-2,\rho_1=-2\,\mathrm{I},\rho_4=1$ in (40) yields the following analytical solution (see Eq. (43) given as in Box VII)

where $\Phi=\frac{143t}{2}+x$.

In Fig. 16, we have demonstrated corresponding dynamic behavior related to the analytical solution obtained in (40) for $\alpha_1=0.48,\alpha_4=0.9,\beta_1=0.2,\beta_4=0.7,\rho_1=0.1,\rho_4=0.1$, and $\sigma=0.48.2,\lambda=0.48.1,\gamma=3.35$. In addition, the sensitivity of this solution is demonstrated based on the responses of two parameters λ and γ in Figs. 17 and 18, respectively. In these diagrams, the high sensitivity of the behavior of the solutions for some values of the parameters is clearly observed.

Category 7: In this case, the following values are retrieved for system solutions

$$\kappa=\frac{4\sqrt{\left(8\gamma^2\lambda\alpha_2^2-16\gamma^2\lambda\alpha_2\alpha_4+8\gamma^2\lambda\alpha_4^2-1\right)\lambda}(\gamma\sigma-1)}{8\gamma^2\lambda\alpha_2^2-16\gamma^2\lambda\alpha_2\alpha_4+8\gamma^2\lambda\alpha_4^2-1},\mu=-\frac{8\lambda\alpha_2^2-16\alpha_4\lambda\alpha_2+8\alpha_4^2\lambda-\sigma^2}{\gamma\sigma-1},$$
$$\sigma=\sigma,\alpha_1=\alpha_2,\alpha_2=\alpha_2,\alpha_3=\alpha_4,\alpha_4=\alpha_4,$$
$$\beta_1=\beta_1,\beta_2=\beta_2,\beta_3=\beta_3,\beta_4=\beta_4,$$
$$\rho_0=-2,\rho_1=\rho_1,\rho_2=\rho_2,\rho_3=\rho_3,\rho_4=\rho_4.\tag{44}$$

Inserting these values into Eq. (7) yields

$$\mathrm{q}(\zeta)=\frac{\left(\rho_1e^{\zeta\alpha_2+\beta_1}+\rho_2e^{\zeta\alpha_2+\beta_2}-\rho_3e^{\zeta\alpha_4+\beta_3}-\rho_4e^{\zeta\alpha_4+\beta_4}\right)^2}{\left(\rho_1e^{\zeta\alpha_2+\beta_1}+\rho_2e^{\zeta\alpha_2+\beta_2}\right)\left(\rho_3e^{\zeta\alpha_4+\beta_3}+\rho_4e^{\zeta\alpha_4+\beta_4}\right)}.\tag{45}$$

So, we get

$$\mathscr{Q}\,(\zeta)=\frac{2\left(\alpha_2-\alpha_4\right)\left(\rho_1e^{\zeta\alpha_2+\beta_1}+\rho_2e^{\zeta\alpha_2+\beta_2}+\rho_3e^{\zeta\alpha_4+\beta_3}+\rho_4e^{\zeta\alpha_4+\beta_4}\right)}{\rho_1e^{\zeta\alpha_2+\beta_1}+\rho_2e^{\zeta\alpha_2+\beta_2}-\rho_3e^{\zeta\alpha_4+\beta_3}-\rho_4e^{\zeta\alpha_4+\beta_4}}.$$

Hence, we obtain an analytical solution to the equation as follows

$$\mathscr{Q}_7\,(x,t)=\frac{2\left(\alpha_2-\alpha_4\right)\left(\rho_1e^{\zeta\alpha_2+\beta_1}+\rho_2e^{\zeta\alpha_2+\beta_2}+\rho_3e^{\zeta\alpha_4+\beta_3}+\rho_4e^{\zeta\alpha_4+\beta_4}\right)}{\rho_1e^{\zeta\alpha_2+\beta_1}+\rho_2e^{\zeta\alpha_2+\beta_2}-\rho_3e^{\zeta\alpha_4+\beta_3}-\rho_4e^{\zeta\alpha_4+\beta_4}}\times e^{i\Phi(x,t)},\tag{46}$$

where

$$\zeta=\frac{\sqrt{8}\sqrt{\lambda\left(-\frac{1}{8}+\gamma^2(\alpha_2-\alpha_4)^2\lambda\right)}\left(\gamma^2\sigma^2x+\left(8t(\alpha_2-\alpha_4)^2\lambda+\sigma^2t-2\sigma x\right)\gamma-2\sigma t+x\right)}{2(\gamma\sigma-1)\left(-\frac{1}{8}+\gamma^2(\alpha_2-\alpha_4)^2\lambda\right)},$$
$$\Phi=-\frac{\left(8\lambda\alpha_2^2-16\alpha_4\lambda\alpha_2+8\alpha_4^2\lambda-\sigma^2\right)t}{\gamma\sigma-1}+\sigma x.\tag{47}$$

Further, solution (46) covers abundant analytical solutions for the main equation, which are described below.

Sub-family 1: Considering the case of $\gamma=1,\lambda=1,\sigma=\frac{1}{2},\alpha_2=-1,\alpha_4=1,\beta_1=-1,\beta_2=-2,\beta_3=-1,\beta_4=-2,\rho_1=1,\rho_2=0,\rho_3=0,\rho_4=-1$ in (46) yields the following analytical solution (see Eq. (48) given as in Box VIII)

where $\Phi=\frac{127t}{2}+\frac{x}{2}$.

Sub-family 2: Considering the case of $\gamma=-1,\lambda=2,\sigma=1,\alpha_2=-1,\alpha_4=1,\beta_1=-1,\beta_2=-2,\beta_3=-1,\beta_4=-2,\rho_1=-1,\rho_2=0,\rho_3=0,\rho_4=1$ in

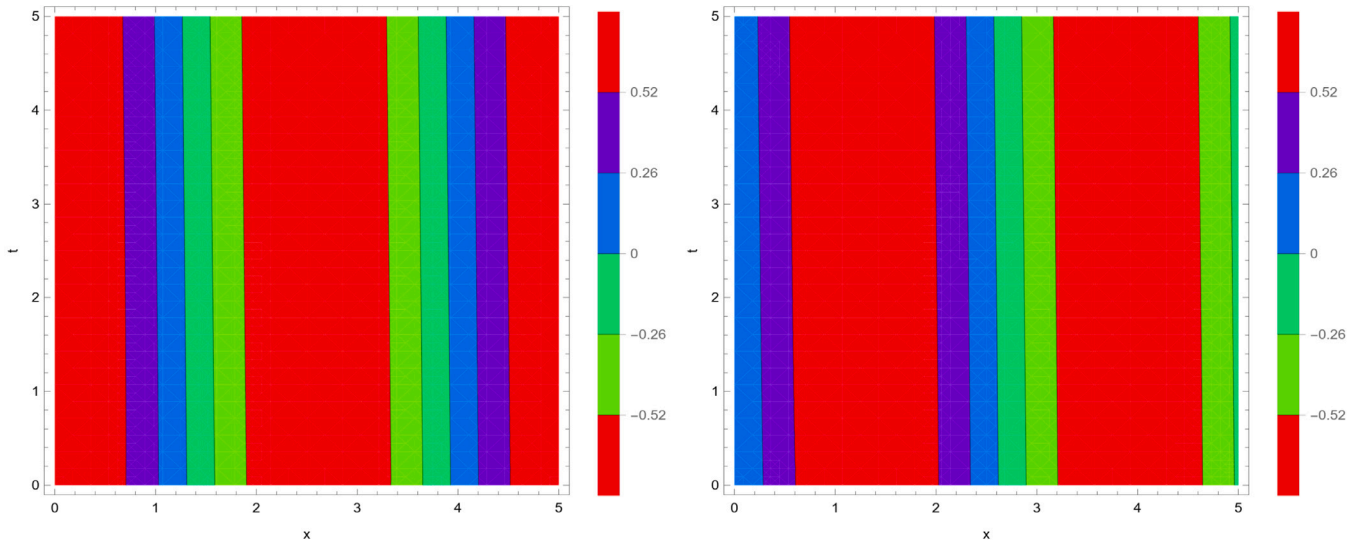

Fig. 16. The wave solution $\mathscr{Q}_6(x,t)$ given by (40). **Left:** Real part, **Right:** Imaginary part.

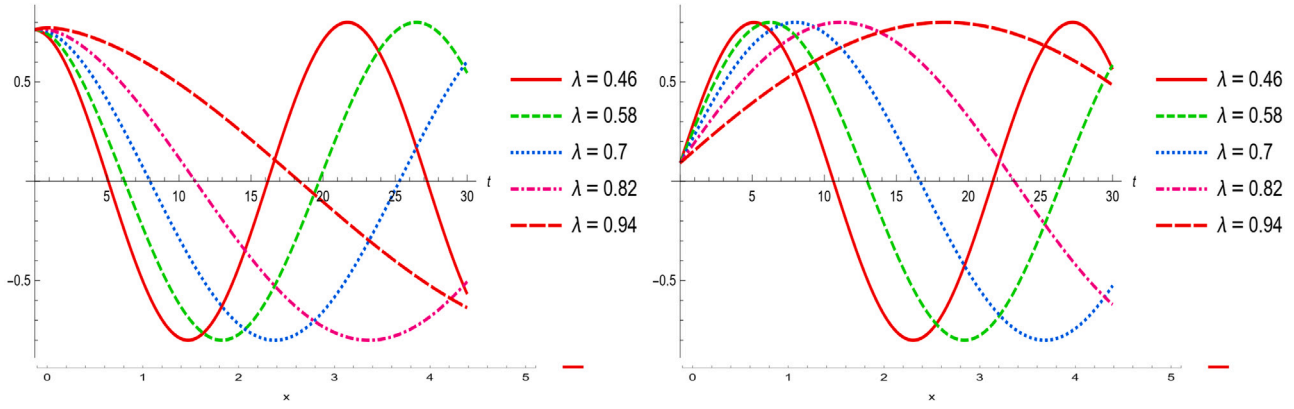

Fig. 17. The effects of λ on $\mathscr{Q}_6(x=0.1,t)$ given by (40) for $\gamma = 1.1$. **Left:** Real part, **Right:** Imaginary part.

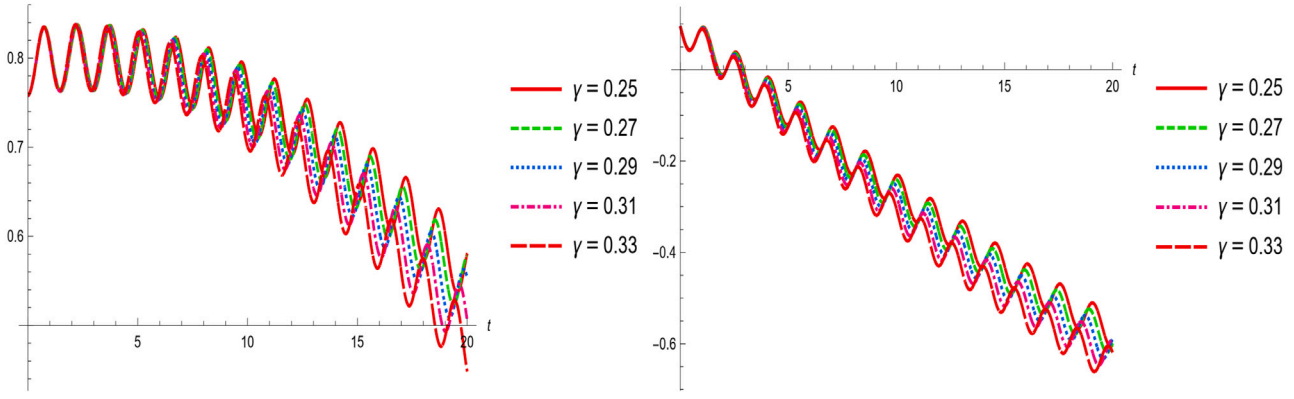

Fig. 18. The effects of γ on $\mathscr{Q}_6(x=0.1,t)$ given by (40) for $\lambda = 1.5$. **Left:** Real part, **Right:** Imaginary part.

$$\mathscr{Q}_{7,1}(x,t) = \frac{-4\cosh\left(-1+\frac{(250t+2x)\sqrt{31}}{31}\right) - 4\sinh\left(-1+\frac{(250t+2x)\sqrt{31}}{31}\right) + 4\cosh\left(2+\frac{(250t+2x)\sqrt{31}}{31}\right) - 4\sinh\left(2+\frac{(250t+2x)\sqrt{31}}{31}\right)}{\cosh\left(-1+\frac{(250t+2x)\sqrt{31}}{31}\right) + \sinh\left(-1+\frac{(250t+2x)\sqrt{31}}{31}\right) + \cosh\left(2+\frac{(250t+2x)\sqrt{31}}{31}\right) - \sinh\left(2+\frac{(250t+2x)\sqrt{31}}{31}\right)} \times e^{i\Phi}. \tag{48}$$

Box VIII.

$$\mathcal{Q}_{7,2}(x,t)=\frac{-4\cosh\left(1+\frac{(134t-8x)\sqrt{14}}{21}\right)+4\sinh\left(1+\frac{(134t-8x)\sqrt{14}}{21}\right)+4\cosh\left(-2+\frac{(134t-8x)\sqrt{14}}{21}\right)+4\sinh\left(-2+\frac{(134t-8x)\sqrt{14}}{21}\right)}{\cosh\left(1+\frac{(134t-8x)\sqrt{14}}{21}\right)-\sinh\left(1+\frac{(134t-8x)\sqrt{14}}{21}\right)+\cosh\left(-2+\frac{(134t-8x)\sqrt{14}}{21}\right)+\sinh\left(-2+\frac{(134t-8x)\sqrt{14}}{21}\right)}\times e^{i\Phi}, \tag{49}$$

Box IX.

(46) yields the following analytical solution (see Eq. (49) given as in Box IX)

where $\Phi = e^{I\left(\frac{63t}{2}+x\right)}$.

In order to validate all the extracted solutions, we inserted them in the corresponding equation to make sure that all of them were correct. Fortunately, all of these solutions were valid from this point of view. Moreover, all necessary symbolic calculations in this manuscript, along with drawing diagrams, have been done using Wolfram Mathematica 12.0.

Conclusion

Recent advances in computers and numerical software have been a great help to researchers in developing evolutionary methods for solving partial equations with partial derivatives. There are many methods in the literature that rely entirely on the use of expensive, complex, and time-consuming calculations in computers. This paper employs an efficient logarithmic transformation technique to obtain some oblique optical solutions to a nonlinear Schrödinger equation of unstable type. This variant form of the Schrödinger equation describes the disturbance of time period in slightly stable and unstable media and manages the instabilities of lossless symmetric two stream plasma and two layer baroclinic. The method used in this article is quite straightforward which offers the explicit expressions of solutions in terms of elementary functions like exponential function. Moreover, it has less computational complexity than some existing methods, and this is one of the highlights of this method. Numerical simulations also complement the analytical findings. Also, to demonstrate the effects of two existing parameters in the model we have plotted 2D profiles. The approach can be used to find novel exact solutions to a wide class of nonlinear differential equations in mathematical physics that will be one of our next goals in future research.

CRediT authorship contribution statement

Yan Cao: Conceptualization, Methodology, Writing – review & editing. **Hayder A. Dhahad:** Writing – review & editing. **Fahd Jarad:** Formal analysis, Methodology, Software, Visualization. **Kamal Sharma:** Investigation, Visualization. **Ali A. Rajhi:** Conceptualization, Investigation, Software, Visualization. **A.S. El-Shafay:** Conceptualization, Formal analysis, Investigation, Methodology, Software, Visualization. **Shima Rashidi:** Software, Writing – original draft. **Shahram Rezapour:** Methodology, Visualization, Writing – review & editing. **S.A. Najati:** Software, Writing – original draft. **Ayman A. Aly:** Conceptualization, Investigation. **Abdulaziz H. Alghtani:** Visualization, Writing – review & editing. **Muhammad Bilal Riaz:** Conceptualization, Formal analysis, Investigation, Software, Writing – original draft.

Declaration of competing interest

The authors declare that they have no known competing financial interests or personal relationships that could have appeared to influence the work reported in this paper.

Acknowledgments

This work was supported by Taif University Researches Supporting Project number (TURSP- 2020/349), Taif University, Taif, Saudi Arabia. The work has been also supported by the Polish National Science Centre under the grant OPUS 18 No. 2019/35/B /ST8/00980. We would like to express our special thanks to **Professor Fabio Baronio**, the editor of the journal for his kind supports, and anonymous referees for their valuable suggestions and advisory comments improving the quality of this paper. The authors have read and agreed to the published version of the manuscript.

References

[1] Folland GB. Introduction to partial differential equations. Princeton University Press; 1995.
[2] Wazwaz AM. Partial differential equations and solitary waves theory. Springer Science & Business Media; 2010.
[3] Gao W, Senel M, Yel G, Baskonus HM, Senel B. New complex wave patterns to the electrical transmission line model arising in network system. Aims Math 2020;5(3):1881–92.
[4] Olver PJ. Introduction to partial differential equations. New York, NY, USA: Springer; 2014.
[5] Ghanbari B, Inc M. A new generalized exponential rational function method to find exact special solutions for the resonance nonlinear Schrödinger equation. Eur Phys J Plus 2018;133:142.
[6] Osman MS, Ghanbari B. New optical solitary wave solutions of fokas-lenells equation in presence of perturbation terms by a novel approach. Optik 2018;175:328–33.
[7] Ghanbari B, Raza N. An analytical method for soliton solutions of perturbed Schrödinger equation with quadratic-cubic nonlinearity. Modern Phys Lett B 2019;33.
[8] Kumar S, Kumar A, Wazwaz AM. New exact solitary wave solutions of the strain wave equation in microstructured solids via the generalized exponential rational function method. Eur Phys J Plus 2020;135(11):1–7.
[9] Ghanbari B, Nisar KS, Aldhaifallah M. Abundant solitary wave solutions to an extended nonlinear Schrödinger's equation with conformable derivative using an efficient integration method. Adv Difference Equ 2020;2020(1):1–25.
[10] Kumar D, Kumar S. Solitary wave solutions of pZK equation using Lie point symmetries. Eur Phys J Plus 2020;135(2):162.
[11] Ghanbari B. On novel nondifferentiable exact solutions to local fractional Gardner's equation using an effective technique. Math Methods Appl Sci.
[12] Ghanbari B. Employing hirota's bilinear form to find novel lump waves solutions to an important nonlinear model in fluid mechanics. Results Phys 2021;29:104689.
[13] Ghanbari B. New analytical solutions for the oskolkov-type equations in fluid dynamics via a modified methodology. Results Phys 2021;28:104610.
[14] Ghanbari B, Kuo C-K. Abundant wave solutions to two novel KP-like equations using an effective integration method. Phys Scr 2021;96:045203.
[15] Ghanbari B, Baleanu D, Qurashi MA. New exact solutions of the generalized benjamin-bona-mahony equation. Symmetry 2018;11:20.
[16] Ghanbari B. Abundant soliton solutions for the hirota-maccari equation via the generalized exponential rational function method. Modern Phys Lett B 2019;33:1950106.
[17] Ghanbari B. Abundant exact solutions to a generalized nonlinear schrödinger equation with local fractional derivative. Math Methods Appl Sci 2021;44:8759–74.
[18] Ghanbari B, Yusuf A, Inc M, Baleanu D. The new exact solitary wave solutions and stability analysis for the (2+1)-dimensional zakharov-kuznetsov equation. Adv Difference Equ 2019;2019.
[19] Ghanbari B, Inc M, Rada L. Solitary wave solutions to the tzitzéica type equations obtained by a new efficient approach. J Appl Anal Comput 2019;9:568–89.
[20] Rahman G, Nisar KS, Ghanbari B, Abdeljawad T. On generalized fractional integral inequalities for the monotone weighted chebyshev functionals. Adv Difference Equ 2020;2020.

[21] Ghanbari B, Kuo C-K. A variety of solitary wave solutions to the (2+1)-dimensional bidirectional SK and variable-coefficient SK equations. Results Phys 2020;18:103266.

[22] Ghanbari B, Kumar S, Niwas M, Baleanu D. The lie symmetry analysis and exact jacobi elliptic solutions for the kawahara-KdV type equations. Results Phys 2021;23:104006.

[23] Kuo C-K, Ghanbari B. On novel resonant multi-soliton and wave solutions to the (3+1)-dimensional GSWE equation via three effective approaches. Results Phys 2021;26:104421.

[24] Ghanbari B, Baleanu D. New optical solutions of the fractional gerdjikov-ivanov equation with conformable derivative. Front Phys 2020;8.

[25] Olver PJ, Rosenau P. The construction of special solutions to partial differential equations. Physics Letters A 1986;114(3):107–12.

[26] Yel G, Baskonus HM, Gao W. New dark-bright soliton in the shallow water wave model. AIMS Math 2020;5(4):4027–44.

[27] Silambarasan R, Baskonus HM, Vijay Anand R, Dinakaran M, Balusamy B, Gao W. Longitudinal strain waves propagating in an infinitely long cylindrical rod composed of generally incompressible materials and it's Jacobi elliptic function solutions. Math Comput Simulation 2021;182:566–602.

[28] Yang XJ, Tenreiro Machado JA, Baleanu D, Cattani C. On exact traveling-wave solutions for local Korteweg–de Vries equation. Chaos, Interdiscip J Nonlin Sci 2016;26(8):084312.

[29] Kayum MA, Akbar MA, Osman MS. Competent closed form soliton solutions to the nonlinear transmission and the low-pass electrical transmission lines. Eur Phys J Plus 2020;135(7):1–20.

[30] Ghanbari B, Baleanu D. A novel technique to construct exact solutions for nonlinear partial differential equations. Eur Phys J Plus 2019;134(10):1–21.

[31] Gao W, Yel G, Baskonus HM, Cattani C. Complex solitons in the conformable (2+1)-dimensional Ablowitz-Kaup-Newell-Segur equation. Aims Math. 2020;5(1):507–21.

[32] Ghanbari B, Akgül A. Abundant new analytical and approximate solutions to the generalized schamel equation. Phys Scr 2020;95(7):075201.

[33] Liu X, Zhang G, Li J, Shi G, Zhou M, Huang B, Tang Y, Song X, Yang W. Deep learning for Feynman's path integral in strong-field time-dependent dynamics. Phys Rev Lett 2020;124:113202.

[34] Yang W, Lin Y, Chen X, Xu Y, Zhang H, Ciappina M, Song X. Wave mixing and high-harmonic generation enhancement by a two-color field driven dielectric metasurface [invited]. Chin Opt Lett 2021;19:123202.

[35] Chen J, Liu Y, Xiang Y, Sood K. Rpptd: robust privacy-preserving truth discovery scheme. IEEE Syst J 2021;1–8.

[36] Wang P, Liu Y. SEMA, Secure and efficient message authentication protocol for VANETs. IEEE Syst J 2021;15:846–55.

[37] Y XU, Meng L, Su LChenXiaojingChenXi, Yuan L, Shi W, Huang G. A strategy to significantly improve the classification accuracy of LIBS data, application for the determination of heavy metals in tegillarca granosa. Plasma Sci Technol 2021;23:085503.

[38] Wu Z, Li C, Cao J, Ge Y. On scalability of association-rule-based recommendation. ACM Trans Web 2020;14:1–21.

[39] Wu Z, Song A, Cao J, Luo J, Zhang L. Efficiently translating complex SQL query to MapReduce jobflow on cloud. IEEE Trans Cloud Comput 2020;8:508–17.

[40] XuXu X, Nieto-Vesperinas M. Azimuthal imaginary poynting momentum density. Phys Rev Lett 2019;123:233902.

[41] Meng F, Pang A, Dong X, Han C, Sha X. H_∞ Optimal performance design of an unstable plant under bode integral constraint. Complexity 2018;2018:1–10.

[42] Sun L, Li C, Zhang C, Liang T, Zhao Z. The strain transfer mechanism of fiber bragg grating sensor for extra large strain monitoring. Sensors 2019;19:1851.

[43] Zhong Q, Yang J, Shi K, Zhong S, Li Z, Sotelo MA. Event-triggered H_∞ load frequency control for multi-area nonlinear power systems based on non-fragile proportional integral control strategy. IEEE Trans Intell Transport Syst 2021;1–11.

[44] Wang K, Li S. Robust distributed modal regression for massive data. Comput Statist Data Anal 2021;160:107225.

[45] Wang K, Wang H, Li S. Renewable quantile regression for streaming datasets. Knowl-Based Syst 2022;235:107675.

[46] Lü X, Chen S-J. Interaction solutions to nonlinear partial differential equations via Hirota bilinear forms, one-lump-multi-stripe and one-lump-multi-soliton types. Nonlin Dyn 2021;103:947–77.

[47] Lü X, Hua Y-F, Chen S-J, Tang X-F. Integrability characteristics of a novel (2+1)-dimensional nonlinear model, Painlevé analysis, soliton solutions, Bäcklund transformation, Lax pair and infinitely many conservation laws. Commun Nonlinear Sci Numer Simul 2021;95:105612.

[48] Lü X, Chen S-J. New general interaction solutions to the KPI equation via an optional decoupling condition approach. Commun Nonlinear Sci Numer Simul 2021;103:105939.

[49] He X-J, Lü X, Li M-G. Bäcklund Transformation, pfaffian, wronskian and grammian solutions to the (3+1)-dimensional generalized Kadomtsev–Petviashvili equation. Anal Math Phys 2020;11.

[50] Chen S-J, Lü X, Tang X-F. Novel evolutionary behaviors of the mixed solutions to a generalized Burgers equation with variable coefficients. Commun Nonlinear Sci Numer Simul 2021;95:105628.

[51] Kallel W, Almusawa H, Mirhosseini-Alizamini SM, Eslami H, Osman MS. Optical soliton solutions for the coupled conformable Fokas–Lenells equation with spatio-temporal dispersion. Results Phys 2021;26:104388.

[52] Akinyemi L, Mẹnol M, Mirzazadeh M, Eslami M. Optical solitons for weakly nonlocal Schrödinger equation with parabolic law nonlinearity and external potential. Optik 2021;230:166281.

[53] Rezazadeh H, Kumar D, Neirameh A, Eslami M, Mirzazadeh M. Applications of three methods for obtaining optical soliton solutions for the Lakshmanan–Porsezian–Daniel model with Kerr law nonlinearity. Pramana - J Phys 2020;94.

[54] Eslami M, Neyrame A, Ebrahimi M. Explicit solutions of nonlinear (2+1)-dimensional dispersive long wave equation. J King Saud Univ Sci 2012;24:69–71.

[55] Braun J, Sambridge M. A numerical method for solving partial differential equations on highly irregular evolving grids. Nature 1995;376(6542):655–60.

[56] Schiesser WE. Pde boundary conditions from minimum reduction of the PDE. Appl Numer Math 1996;20(1–2):171–9.

[57] Ghanbari B. On approximate solutions for a fractional prey–predator model involving the Atangana–Baleanu derivative. Adv Difference Equ 2020;2020(1):1–24.

[58] Holmström M. Solving hyperbolic PDEs using interpolating wavelets. SIAM J Sci Comput 1999;21(2):405–20.

[59] Beckett G, Mackenzie JA, Ramage A, Sloan DM. On the numerical solution of one-dimensional PDEs using adaptive methods based on equidistribution. J. Comput Phys 2001;167(2):372–92.

[60] Beilina L, Klibanov MV. A globally convergent numerical method for a coefficient inverse problem. SIAM J Sci Comput 2008;31(1):478–509.

[61] Roshani M, Phan GT, Ali PJM, Roshani GH, Hanus R, Duong T, et al. Evaluation of flow pattern recognition and void fraction measurement in two phase flow independent of oil pipeline's scale layer thickness. Alex Eng J 2021;60:1955–66.

[62] Roshani M, Phan G, Roshani GH, Hanus R, Nazemi B, Corniani E, et al. Combination of x-ray tube and GMDH neural network as a nondestructive and potential technique for measuring characteristics of gas-oil-water three phase flows. Measurement 2021;168:108427.

[63] Roshani M, Phan G, Faraj RH, Phan N-H, Roshani GH, Nazemi B, et al. Proposing a gamma radiation based intelligent system for simultane- ous analyzing and detecting type and amount of petroleum by-products. Nucl Eng Technol 2021;53:1277–83.

[64] Roshani M, Sattari MA, Ali PJM, Roshani GH, Nazemi B, Corniani E, et al. Application of GMDH neural network technique to improve measuring precision of a simplified photon attenuation based two-phase flowmeter. Flow Meas Instrum 2020;75:101804.

[65] Sattari MA, Roshani GH, Hanus R, Nazemi E. Applicability of time-domain feature extraction methods and artificial intelligence in two-phase flow meters based on gamma-ray absorption technique. Measurement 2021;168:108474.

[66] Roshani G, Hanus R, Khazaei A, Zych M, Nazemi E, Mosorov V. Density and velocity determination for single-phase flow based on radiotracer technique and neural networks. Flow Meas Instrum 2018;61:9–14.

[67] Karami A, Roshani GH, Khazaei A, Nazemi E, Fallahi M. Investigation of different sources in order to optimize the nuclear metering system of gas-oil-water annular flows. Neural Comput Appl 2018;32:3619–31.

[68] Karami A, Roshani GH, Nazemi E, Roshani S. Enhancing the performance of a dual-energy gamma ray based three-phase flow meter with the help of grey wolf optimization algorithm. Flow Meas Instrum 2018;64:164–72.

[69] Nazemi E, Roshani G, Feghhi S, Setayeshi S, Zadeh EE, Fatehi A. Optimization of a method for identifying the flow regime and measuring void fraction in a broad beam gamma-ray attenuation technique. Int J Hydrogen Energy 2016;41:7438–44.

[70] Roshani GH, Nazemi E, Roshani MM. Flow regime independent volume fraction estimation in three-phase flows using dual-energy broad beam technique and artificial neural network. Neural Comput Appl 2016;28:1265–74.

[71] Roshani GH, Roshani S, Nazemi E, Roshani S. Online measuring density of oil products in annular regime of gas-liquid two phase flows. Measurement 2018;129:296–301.

[72] Roshani G, Nazemi E, Roshani M. Intelligent recognition of gas-oil-water three-phase flow regime and determination of volume fraction using radial basis function. Flow Meas Instrum 2017;54:39–45.

[73] Nazemi E, Feghhi S, Roshani G, Peyvandi RG, Setayeshi S. Precise void fraction measurement in two-phase flows independent of the flow regime using gamma-ray attenuation. Nucl Eng Technol 2016;48:64–71.

[74] Roshani G, Nazemi E, Roshani M. Identification of flow regime and estimation of volume fraction independent of liquid phase density in gas-liquid two-phase flow. Prog Nucl Energy 2017;98:29–37.

[75] Roshani G, Nazemi E, Feghhi S, Setayeshi S. Flow regime identification and void fraction prediction in two-phase flows based on gamma ray attenuation. Measurement 2015;62:25–32.

[76] Roshani G, Nazemi E, Feghhi S. Investigation of using 60 co source and one detector for determining the flow regime and void fraction in gas-liquid two-phase flows. Flow Meas Instrum 2016;50:73–9.

[77] Roshani G, Feghhi S, Mahmoudi-Aznaveh A, Nazemi E, Adineh-Vand A. Precise volume fraction prediction in oil-water-gas multiphase flows by means of gamma-ray attenuation and artificial neural networks using one detector. Measurement 2014;51:34–41.
[78] Roshani G, Nazemi E. Intelligent densitometry of petroleum products in stratified regime of two phase flows using gamma ray and neural network. Flow Meas Instrum 2017;58:6–11.
[79] Roshani G, Nazemi E, Roshani M. Usage of two transmitted detectors with optimized orientation in order to three phase flow metering. Measurement 2017;100:122–30.
[80] Rezazadeh H, Korkmaz A, Khater MMA, Eslami M, Lu D, Attia RAM. New exact traveling wave solutions of biological population model via the extended rational sinh-cosh method and the modified Khater method. Modern Phys Lett B 2019;33:1950338.
[81] Khalil R, Al Horani M, Yousef A, Sababheh M. A new definition of fractional derivative. J Comput Appl Math 2014;264:65–70.
[82] Atangana A, Baleanu D, Alsaedi A. Analysis of time-fractional Hunter-Saxton equation, a model of neumatic liquid crystal. Open Phys 2016;14(1):145–9.
[83] Podlubny I. Fractional differential equations, an introduction to fractional derivatives, fractional differential equations, to methods of their solution and some of their applications. Amsterdam: Elsevier; 1998.
[84] Hilfer R. Fractional diffusion based on Riemann–Liouville fractional derivatives. J Phys Chem B 2000;104(16):3914–7.
[85] Caputo M, Fabrizio M. A new definition of fractional derivative without singular kernel. Progr Fract Differ Appl 2015;1(2):1–3.
[86] Abdon A, Baleanu D. New fractional derivatives with nonlocal and non-singular kernel, theory and application to heat transfer model. Therm Sci 2016;20(2):763–9.
[87] Ghanbari B. On the modeling of the interaction between tumor growth and the immune system using some new fractional and fractional-fractal operators. Adv Difference Equ 2020;2020(1):1–32.
[88] Ghanbari B, Kumar D. Numerical solution of predator–prey model with Beddington–DeAngelis functional response and fractional derivatives with Mittag-Leffler kernel. Chaos, Interdiscip J Nonlin Sci 2019;29(6):063103.
[89] Souna F, Lakmeche A, Djilali S. The effect of the defensive strategy taken by the prey on predator–prey interaction. J Appl Math Comput 2020;64(1):665–90.
[90] Ghanbari B, Kumar S, Kumar R. A study of behaviour for immune and tumor cells in immunogenetic tumour model with non-singular fractional derivative. Chaos Solitons Fractals 2020;133(1):109619.
[91] Djilali S. Pattern formation of a diffusive predator–prey model with herd behavior and nonlocal prey competition. Math Methods Appl Sci 2020;43(5):2233–50.
[92] Ghanbari B, Atangana A. Some new edge detecting techniques based on fractional derivatives with non-local and non-singular kernels. Adv Difference Equ 2020;2020(1):1–9.
[93] Ghanbari B. A fractional system of delay differential equation with non-singular kernels in modeling hand-foot-mouth disease. Adv Difference Equ 2020;2020(1):1–20.
[94] Odibat Z. Approximations of fractional integrals and Caputo fractional derivatives. Appl Math Comput 2006;178(2):527–33.
[95] Ghanbari B. On the modeling of an eco-epidemiological model using a new fractional operator. Results Phys 2021;21:103799.
[96] Ghanbari B, Gómez-Aguilar J. Modeling the dynamics of nutrient-phytoplankton-zooplankton system with variable-order fractional derivatives. Chaos Solitons Fractals 2018;116:114–20.
[97] Ghanbari B. On fractional approaches to the dynamics of a SARS-CoV-2 infection model including singular and non-singular kernels. Results Phys 2021;28:104600.
[98] Ghanbari B, Cattani C. On fractional predator and prey models with mutualistic predation including non-local and nonsingular kernels. Chaos Solitons Fractals 2020;136:109823.
[99] Srivastava HM, Günerhan H, Ghanbari B. Exact traveling wave solutions for resonance nonlinear schrödinger equation with intermodal dispersions and the kerr law nonlinearity. Math Methods Appl Sci 2019;42:7210–21.
[100] Nabti A, Ghanbari B. Global stability analysis of a fractional SVEIR epidemic model. Math Methods Appl Sci 2021;44:8577–97.
[101] Bu W, Xiao A. An h-p version of the continuous petrov-galerkin finite element method for riemann-liouville fractional differential equation with novel test basis functions. Numer Algorithms 2018;81:529–45.
[102] Zang Y, Bao G, Ye X, Zhou H. Weak adversarial networks for high-dimensional partial differential equations. J Comput Phys 2020;411:109409.
[103] Ghanbari B, Günerhan H, Srivastava H. An application of the atangana-baleanu fractional derivative in mathematical biology: A three-species predator–prey model. Chaos Solitons Fractals 2020;138:109910.
[104] Ghanbari B, Djilali S. Mathematical analysis of a fractional-order predator–prey model with prey social behavior and infection developed in predator population. Chaos Solitons Fractals 2020;138:109960.
[105] Ghanbari B. On forecasting the spread of the COVID-19 in iran: The second wave. Chaos Solitons Fractals 2020;140:110176.
[106] Djilali S, Ghanbari B. Coronavirus pandemic, a predictive analysis of the peak outbreak epidemic in South Africa, Turkey, and Brazil. Chaos Solitons Fractals 2020;138:109971.
[107] Ghanbari B, Atangana A. A new application of fractional atangana-baleanu derivatives, designing ABC-fractional masks in image processing. Physica A 2020;542:123516.
[108] Djilali S, Ghanbari B. Dynamical behavior of two predators-one prey model with generalized functional response and time-fractional derivative. Adv Difference Equ 2021;2021.
[109] Djilali S, Ghanbari B. The influence of an infectious disease on a prey-predator model equipped with a fractional-order derivative. Adv Difference Equ 2021;2021.
[110] Ghanbari B. A new model for investigating the transmission of infectious diseases in a prey-predator system using a non-singular fractional derivative. Math Methods Appl Sci 2021.
[111] Ghanbari B. Chaotic behaviors of the prevalence of an infectious disease in a prey and predator system using fractional derivatives. Math Methods Appl Sci 2021;44:9998–10013.
[112] Ghanbari B. On approximate solutions for a fractional prey-predator model involving the atangana-baleanu derivative. Adv Difference Equ 2020;2020.
[113] Ghanbari B. On detecting chaos in a prey-predator model with prey's counter-attack on juvenile predators. Chaos Solitons Fractals 2021;150:111136.
[114] Pawlik M, Rowlands G. The propagation of solitary waves in piezoelectric semiconductors. J Phys C Solid State Phys 1975;21(8):1189.
[115] Arbabi S, Najafi M. Exact solitary wave solutions of the complex nonlinear Schrödinger equations. Optik 2016;127(11):4682–8.
[116] Wadati M, Segur H, Ablowitz MJ. A new Hamiltonian amplitude equation governing modulated wave instabilities. J Phys Soc Japan 1992;(4):1187–93.
[117] Wadati M, Yajima T, Iizuka T. The theory and applications of the unstable nonlinear Schrödinger equation. Chaos Solitons Fractals 1991;1(3):249–71.
[118] Lu D, Seadawy A, Arshad M. Applications of extended simple equation method on unstable nonlinear Schrödinger equations. Optik 2017;140:136–44.
[119] Pandir Y, Ekin A. Dynamics of combined soliton solutions of unstable nonlinear schrodinger equation with new version of the trial equation method. Chinese J Phys 2020;67:534–43.
[120] Arshad M, Seadawy AR, Lu D, Jun W. Modulation instability analysis of modify unstable nonlinear schrodinger dynamical equation and its optical soliton solutions. Results Phys 2017;7:4153–61.
[121] Tala-Tebue E, Seadawy AR, Djoufack ZI. The modify unstable nonlinear Schrödinger dynamical equation and its optical soliton solutions. Opt Quantum Electron 2018;50(10):380.
[122] Arshad M, Seadawy AR, Lu D, Jun W. Optical soliton solutions of unstable non-linear Schröodinger dynamical equation and stability analysis with applications. Optik 2018;157:597–605.
[123] Li Y, Lu D, Arshad M, Xu X. New exact traveling wave solutions of the unstable nonlinear Schrödinger equations and their applications. Optik 2021;226:165386.
[124] Rizvi ST, Seadawy AR, Ahmed S, Younis M, Ali K. Study of multiple lump and rogue waves to the generalized unstable space time fractional nonlinear Schrödinger equation. Chaos Solitons Fractals 2021;151:111251.